

Report

on

SAFETY AUDIT OF THE BRIDGE OVER SPILLWAY OF THE UMIAM CONCRETE DAM

Location

Ri-Bhoi District, Meghalaya

Name of Expert

Dr. Romanbabu Oinam
Assistant Professor

Date of Investigation

22nd July 2023

Completed on

23rd July 2023



Department of Civil Engineering
Indian Institute of Technology Guwahati

August, 2023

Report

on

SAFETY AUDIT OF THE BRIDGE OVER SPILLWAY OF THE UMIAM CONCRETE DAM

Report Prepared by:

Dr. Romanbabu Oinam

Assistant Professor

Email: romanbabu@iitg.ac.in

Phone: 0361-258 3233

Department of Civil Engineering

Indian Institute of Technology Guwahati

Guwahati, Assam-781039

TABLE OF CONTENTS

Table of Contents.....	i
List of Figures.....	ii
List of Tables.....	iv
1.1 Introduction	1
1.1.1 Details of the bridge	1
1.2 Scope of the Work.....	2
1.3 Overview on Tests	2
1.3.1 Visual Observation Based Tests	2
1.3.2 Tests for Quality.....	3
1.3.3 Tests for Strength of Concrete.....	4
1.3.4 Tests for Durability	5
1.4 Results and Discussion	6
1.4.1 Visual Inspection Results	6
1.4.2 Rebound Hammer Results	24
1.4.3 UPV Results.....	26
1.4.4 Core Compression Test Results	29
1.4.5 Half-Cell Potential Test Results.....	32
1.4.6 Carbonation Test Results	33
1.4.7 GPR Scanning Results.....	34
1.5 Conclusions	45
1.5.1 Visual Inspection.....	45
1.5.2 Rebound Hammer Test.....	45
1.5.3 UPV (Ultrasonic Pulse Velocity Test)	45
1.5.4 Core Compression Test	45
1.5.5 Half-Cell Potential Test	46
1.5.6 Carbonation Test	46
1.5.7 GPR Test.....	46
1.6 Recommendations	46

LIST OF FIGURES

Figure 1: Location of the spillway bridge.....	1
Figure 2: Visual inspection and crack mapping carried out on various parts of the structure..	2
Figure 3: Rebound hammer and Ultrasonic pulse velocity test on the bridge abutment	3
Figure 4: Core extraction test and Half cell potential test on bridge abutments.....	4
Figure 5: Carbonation test and Reinforcement scanning carried out on bridge girders	5
Figure 6: Observations on the West side of Abutment-2 and Girder	6
Figure 7: Observations on South-West side Abutment-2	8
Figure 8: Observations on South-East side Abutment-2.....	9
Figure 9: Observations on South side Abutment 2-Pier 1	10
Figure 10: Observations on West side Abutment-2.....	10
Figure 11: Observations on West side Pier 1	11
Figure 12: Observations on West side Abutment-2 and Pier-1	12
Figure 13: Observations on West side Abutment-1 and Pier-1	13
Figure 14: Observations on North side Abutment-1 and Pier-1	14
Figure 15: Observations on East side Abutment 2 and Pier1	18
Figure 16: Observations on South side Abutment-2 and Pier-1	19
Figure 17: Observations on West side Abutment-1 and Pier-1	20
Figure 18: Observations on East and North Pier-1	20
Figure 19: Observations on North side Abutment-1 and Pier-1	21
Figure 20: Observations on East side deck slab and South side diaphragm wall	22
Figure 21: Observations on South side deck slab and North side girder beam	22
Figure 22: Distribution of rebound numbers measured	25
Figure 23: Estimated concrete layer quality based on rebound values	25
Figure 24: Estimated compressive strength based on rebound hammer test	25
Figure 25: Distribution of measured UPV velocity	28

Figure 26: Estimated quality of concrete based on UPV test results	28
Figure 27: Distribution of compressive strength values estimated from core compression test	31
Figure 28: Core concrete compressive strength.....	31
Figure 29: Distribution of half-cell potential values measured from the site	32
Figure 30: Estimated corrosion probability by half cell potential test.....	33
Figure 31: Distribution of depth of carbonation values obtained on various points.....	34
Figure 32: Rebar detection in scan-1 zone (beam)	35
Figure 33: Rebar detection in scan-2 zone (slab).....	36
Figure 34: Rebar detection in scan-3 zone (diaphragm wall)	37
Figure 35: Rebar detection in scan-4 zone (Pier Cap)	38
Figure 36: Rebar detection in scan-5 zone (beam)	39
Figure 37: Rebar detection in scan-6 zone (beam)	40
Figure 38: Rebar detection in scan-7 zone (slab).....	41
Figure 39: Rebar detection in scan-8 zone (beam)	42
Figure 40: Rebar detection in scan-9 zone (slab).....	43
Figure 41: Rebar detection in scan-10 zone (diaphragm wall)	44

LIST OF TABLES

Table 1: Classification of concrete quality ratings based on UPV test IS 516 (Part-5).....	4
Table 2: Half-cell potentiometer test criteria as per IS 516	5
Table 3: Rebound hammer test results	24
Table 4: Ultrasonic pulse velocity test results	26
Table 5: Core compressive test results.....	29
Table 6: Concrete Compressive Strength (Core Test)	30
Table 7: Half-cell potential test results	32
Table 8: Carbonation test results.....	33
Table 9: GPR test results.....	45

SAFETY AUDIT REPORT: BRIDGE OVER SPILLWAY OF THE UMIAM CONCRETE DAM

1.1 Introduction

A spillway bridge located in Umiam Dam, Shillong, Meghalaya, is in used condition (i.e., under heavy traffic). The bridge was constructed in 1965 and is one of the most important bridge in the state of Meghalaya. Therefore, IIT Guwahati did a structural audit to check the stability and strength of the bridge. The details of this investigation report are presented in the subsequent sections.

1.1.1 Details of the bridge

Name of Bridge: Umiam dam spillway bridge

Bridge Location: Shillong route, Meghalaya

Type of Bridge: Spillway concrete dam bridge, girder & Cast in situ deck slab structure

Type of Foundation: Open Foundation

Length of spans: 16.0 m each (*Two span*)

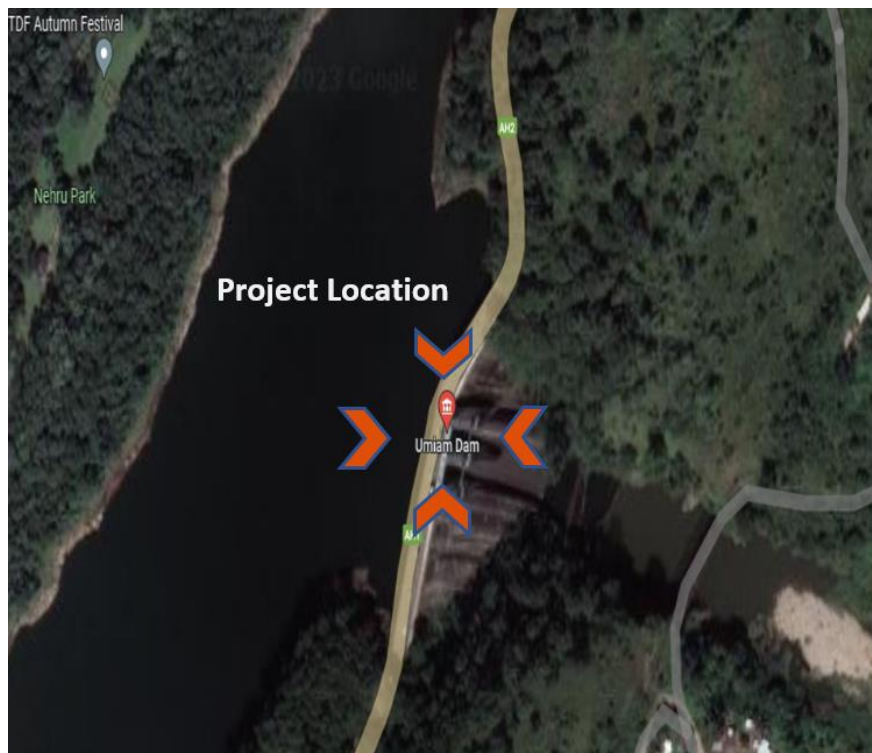


Figure 1: Location of the spillway bridge

1.2 Scope of the Work

- Scope of the work is restricted only to the supper structure of the spillway bridge.
- No Underwater inspection.
- Design and analysis of the bridge are not under scope.

1.3 Overview on Tests

To check the soundness of the structure, the test are classified into four category as (a) visual inspection, (b) quality check, (c) strength check, and (d) durability check. Under the quality check, Ultrasonic pulse velocity test (UPV) and Rebound hammer test are considered. For strength check, Core cutting (compression test) method is used. Incase of durability check, Carbonation depth measurement test, Half cell potential test and Cover test (i.e., ground penetrating scan) are used.

1.3.1 Visual Observation Based Tests

Visual observation-based tests, also known as visual inspection or visual testing, are non-destructive testing methods that rely on the human eye to detect surface defects, anomalies, or irregularities in materials, components, or structures. These tests are widely used across various industries to assess the quality and integrity of structures without causing any damage. This test is often employed as a preliminary screening tool to identify obvious defects before more sophisticated testing methods are employed. Figure 2 shows visual inspection and crack mapping carried out on various parts of the structure.



Figure 2: Visual inspection and crack mapping carried out on various parts of the structure

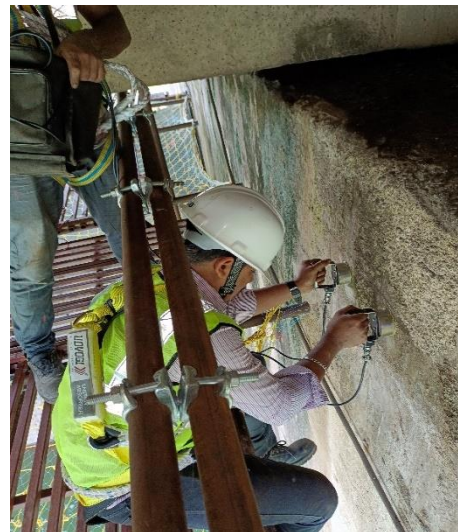
1.3.2 Tests for Quality

1.3.2.1 Rebound hammer test

The rebound hammer test, also known as the Schmidt hammer test, is a non-destructive testing method used to assess concrete or rock's compressive strength or hardness. It is a portable device that measures the rebound of a spring-loaded mass impacting the surface of the material under investigation. The surface hardness, density, and overall strength of the material influence the rebound distance. Figure 3 shows a typical rebound hammer test conducted on the structure. A higher rebound value indicates a harder or stronger material, while a lower rebound value suggests a softer or weaker material. However, it's important to note that the rebound hammer test indirectly measures the strength and is not as accurate as other destructive testing methods, such as compressive strength tests conducted in a laboratory (IS 516 Part 2 Sec 4, BS 1881 Part 202).



Rebound hammer



Ultrasonic Pulse Velocity

Figure 3: Rebound hammer and Ultrasonic pulse velocity test on the bridge abutment

1.3.2.2 Ultrasonic pulse velocity test

The Ultrasonic Pulse Velocity (UPV) test is also a non-destructive testing method used to assess the quality, uniformity, and integrity of concrete, masonry, and other construction materials. It measures the travel time of ultrasonic pulses through the material, providing information about its density, homogeneity, and potential defects. In the UPV test, two piezoelectric transducers are placed on the surface of the material being tested. One transducer emits an ultrasonic pulse, usually in the range of 50 to 54 kHz, while the other transducer acts as a receiver. The pulse travels through the material and is detected by the receiving transducer.

The time pulse travels between the two transducers is recorded. Figure 3 shows the UPV test conducted on the structure. The velocity of the ultrasonic pulse is influenced by the elastic properties of the material, including its density and stiffness. In general, higher velocities indicate materials with higher density and greater integrity. Conversely, lower velocities may suggest the presence of voids, cracks, or other defects that can impede the transmission of the ultrasonic waves. Table 1 shows typical concrete quality ratings based on the UPV test.

Table 1: Classification of concrete quality ratings based on UPV test IS 516 (Part-5)

Sl. No	Pulse Velocity (km/sec)	Concrete Quality (ratings)
i	< 3	Poor
ii	3.0 -3.75	Doubtful
iii	3.75 - 4.40	Good
iv	> 4.40	Excellent

1.3.3 Tests for Strength of Concrete

1.3.3.1 Core cutting and compression test

Concrete core cutting tests, often referred to as core sampling or core drilling, are a non-destructive testing method used to extract cylindrical samples (cores) from hardened concrete structures for the purpose of evaluating the concrete's properties, quality, and integrity. This method provides valuable information about the in-place concrete's composition, strength, durability, and any potential defects (IS 516 Part 4). Figure 4 shows the core extraction process from the structure.



Concrete core cutting



Half cell potential

Figure 4: Core extraction test and Half cell potential test on bridge abutments

1.3.4 Tests for Durability

1.3.4.1 Half-cell potential test

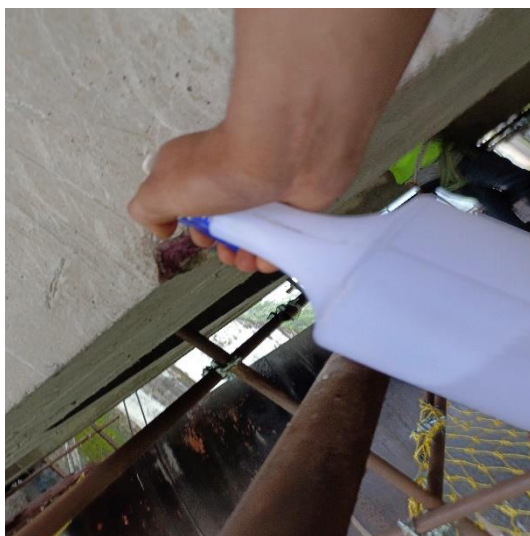
The half-cell potential test, also known as the corrosion potential test or the half-cell potential measurement, is a non-destructive testing method used to assess the likelihood of corrosion occurring in reinforced concrete structures, particularly in the reinforcement bars (rebar). This test provides valuable information about the electrochemical condition of the reinforcing steel within the concrete, which can help identify areas susceptible to corrosion and guide maintenance and repair efforts (BS 1881 Part 201). Table 2 shows the probability of active corrosion ratings based on the Half-cell potential test.

Table 2: Half-cell potentiometer test criteria as per IS 516

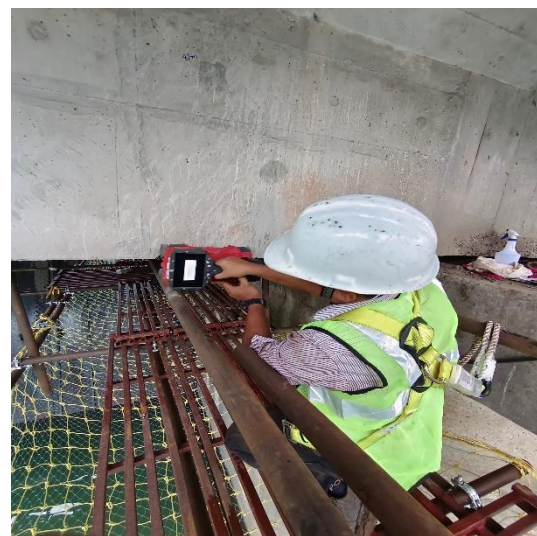
Half Cell Potential Reading (Cu/CuSO ₄)	Probability of Active Corrosion
More positive than -200 mV	10%
Between -200 mV to -350 mV	50%
More negative than -350 mV	90%

1.3.4.2 Carbonation depth measurement test

This is a non-destructive testing method used to assess the extent of carbonation within the surface layer of concrete structures. Carbonation is a chemical reaction between carbon dioxide (CO₂) in the atmosphere and the calcium hydroxide (lime) in the concrete, which leads to the formation of calcium carbonate. This reaction reduces the alkalinity of the concrete,



Carbonation test



GPR test

Figure 5: Carbonation test and Reinforcement scanning carried out on bridge girders

potentially compromising the passivation of reinforcing steel and increasing the risk of corrosion. The carbonation depth measurement test provides valuable information about how far carbonation has penetrated the concrete, which is important for assessing the structure's durability and potential corrosion risk (IS 516 Draft Part 2 Sec 4, EN 14630: 2007). Figure 5 shows the process of the carbonation test on the structure.

1.3.4.3 Ground penetrating scan (GPR scan)

This type of non-destructive testing method is used to assess and inspect subsurface structures, materials, and features without causing any damage. GPR is particularly useful for imaging and identifying anomalies within concrete, soil, rock, and other materials. As an NDT test, GPR provides valuable information without requiring the destruction or alteration of the inspected material, like locating steel rebars or determining the cover and size of bars. Figure 5 shows the process of the GPR test conducted on the structure.

All the above mention tests are conducted on the Umiam spillway bridge. The results of all tests are presented in the subsequent sections.

1.4 Results and Discussion

1.4.1 Visual Inspection Results

As a part of the visual inspection, multiple photographs are taken from different parts of the structure. These photographs are presented location-wise in figures with remarks.



Silt accumulation & minor vegetation growth were observed on the pier cap



Active leakages were observed on the bottom slab soffit

Figure 6: Observations on the West side of Abutment-2 and Girder



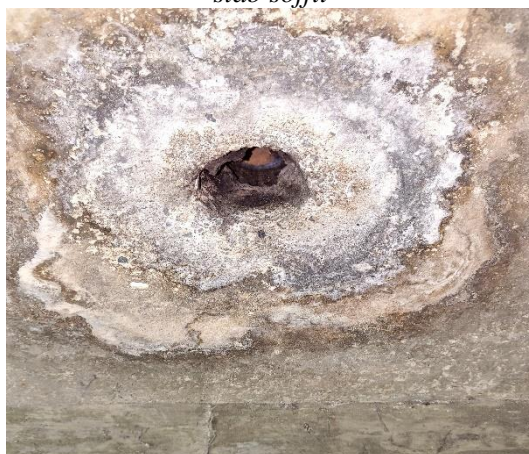
Repair in patches observed on the deck slab & diaphragm wall



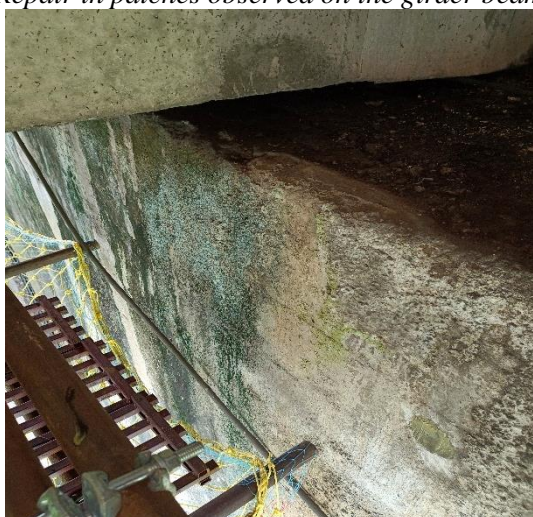
Major Seepages sign was observed on the deck slab soffit



Repair in patches observed on the girder beam



Major Seepages sign on the deck slab soffit



Seepages sign and vegetation growth on pier cap



Seepages sign observed on deck slab surface

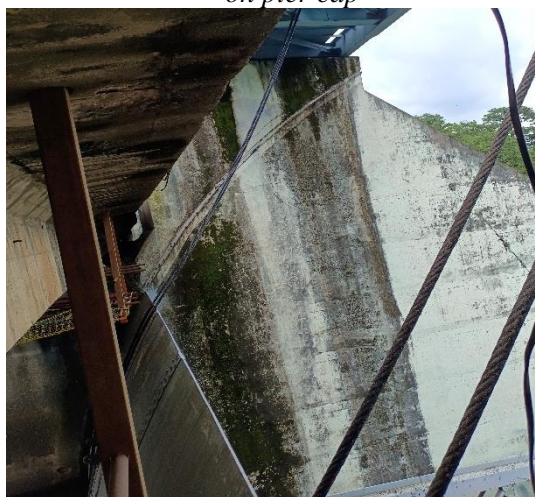
Figure 7: Observations on South-West side Abutment-2 (Continue in Next Page)



Seepages sign & major discoloration observed on pier cap



Repair in patches observed on girder beam



Seepages sign observed on slab soffit



Seepages sign and discoloration observed on spillway wall

Figure 7: Observations on South-West side Abutment-2



Seepages sign observed on slab soffit



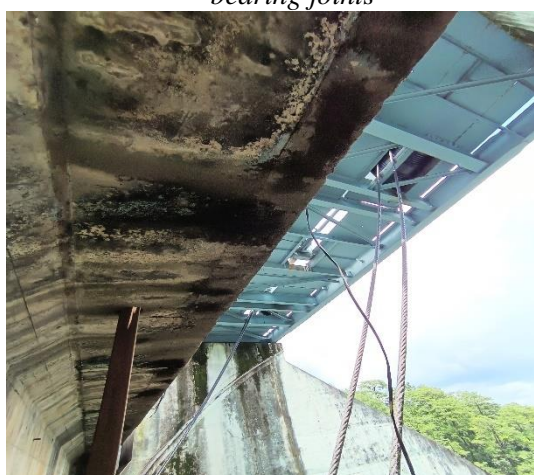
Seepages sign and discoloration observed on spillway wall



Silt accumulation observed on pier cap and bearing joints



Seepages sign observed on slab soffit



Major seepages sign & discoloration observed on slab soffit



Major Seepages sign and discoloration observed on pier cap

Figure 8: Observations on South-East side Abutment-2



Minor Cracks observed on cross girder



Minor Cracks & repair in patches observed on deck slab & diaphragm wall

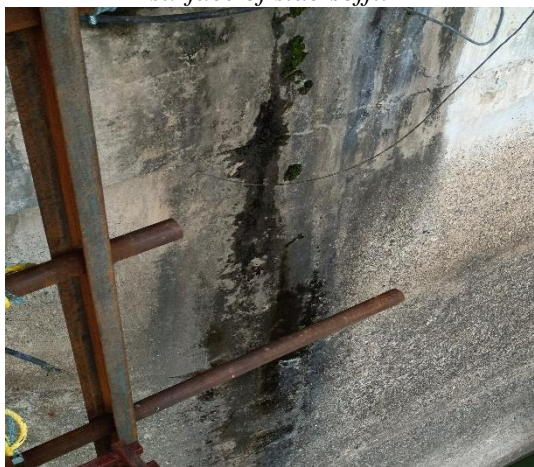
Figure 9: Observations on South side Abutment 2-Pier 1



Major seepages signs observed on bottom surface of slab soffit



Silt accumulation & Vegetation growth observed on pier cap



Moderate Seepages sign, Discoloration observed on pier surface area

Figure 10: Observations on West side Abutment-2



Silt accumulation, vegetation growth & major seepages sign observed on pier cap



Silt accumulation, Major seepages sign & vegetation growth observed



Major vegetation growth, discoloration & rusting in bearing observed



Major seepages sign & spalling observed on bottom of deck slab & girders

Figure 11: Observations on West side Pier 1



Major seepages sign & Discoloration observed on external slab soffit



Major seepages sign observed on deck slab surface

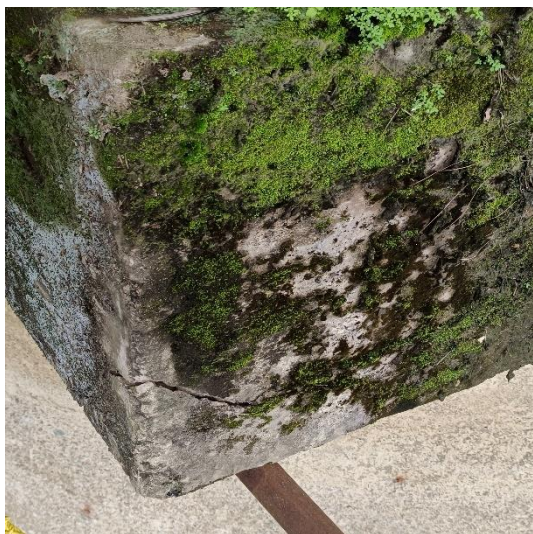


Spalling observed on top surface of cross girders



Repair in patches observed on girder beam & cross girders

Figure 12: Observations on West side Abutment-2 and Pier-1



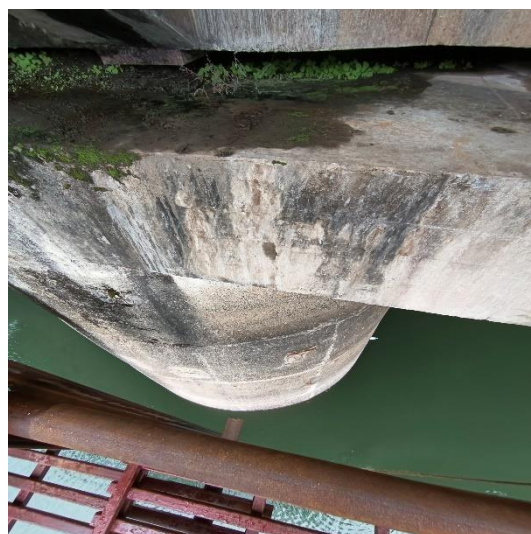
Major vegetation growth, Seepages sign & Cracks observed on pier cap



Major Seepages sign & discoloration observed on deck slab soffit



Seepages sign & discoloration observed on deck slab



Silt accumulation, Vegetation growth and seepages signs observed on bearing junctions

Figure 13: Observations on West side Abutment-1 and Pier-1



Silt accumulation, vegetation growth and seepages sign observed on bearing junctions



Major Seepages signs & discoloration observed on slab soffit

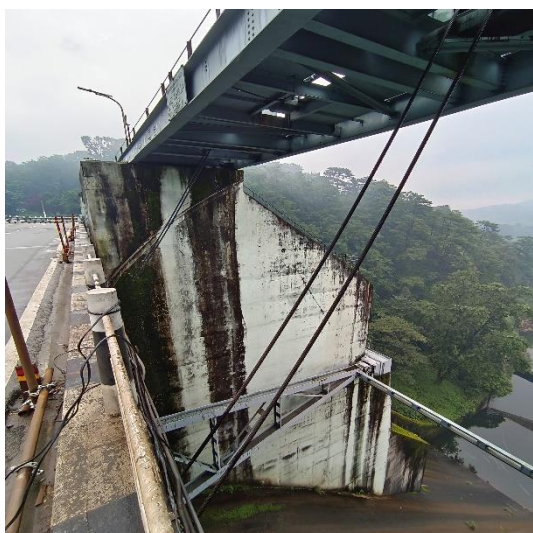


Vegetation growth, Seepages sign & silt accumulation observed on bearing junctions



Moderate Seepages signs observed on deck slab soffit surface

Figure 14: Observations on North side Abutment-1 and Pier-1



Major discoloration due to seepages sign observed on spillway wall



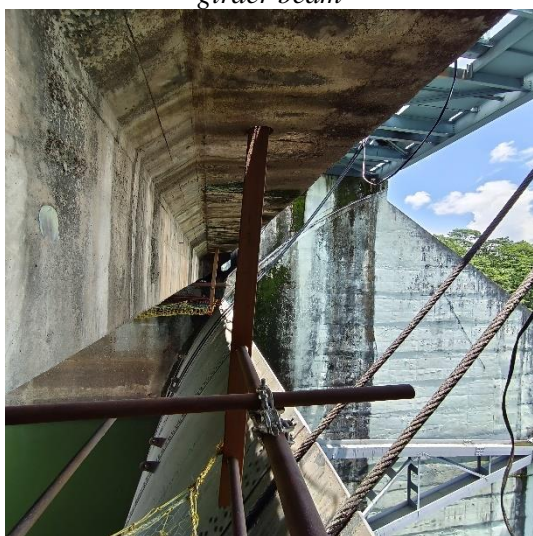
Minor discoloration observed on beam & slab surface area



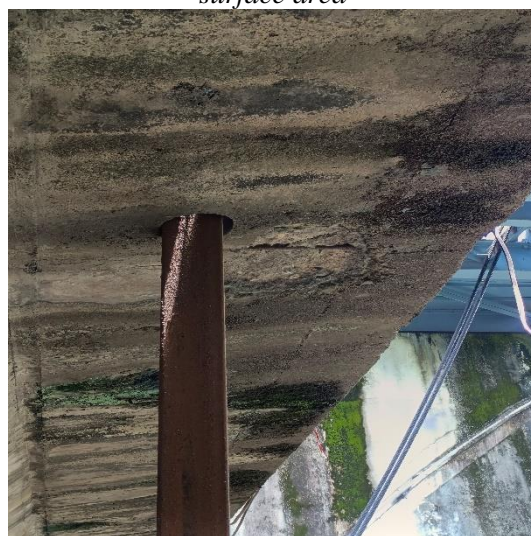
Shear cracks & repair in patches observed on girder beam



Minor discoloration observed on beam & slab surface area



Seepages sign observed on slab soffit



Major seepages sign & spalling observed on slab soffit

Figure 15: Observations on East side Abutment-2 and Pier-1 (Continue in Page: 15-18)



Silt accumulation and seepage signs observed on bearing junctions



Shear cracks observed girder beam surface area



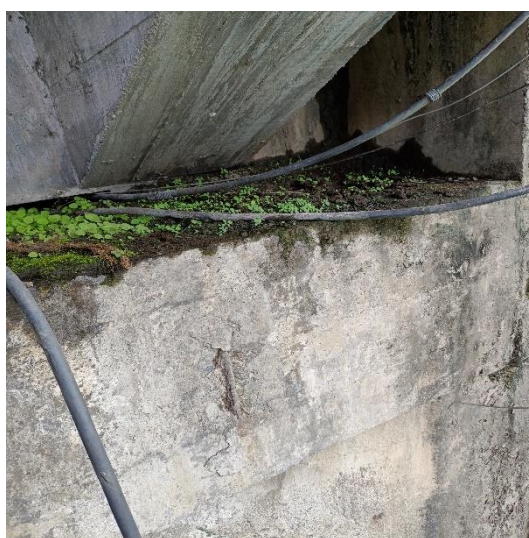
Shear cracks & repair in patches observed on girder beam



Transverse cracks observed on deck slab soffit area



Transverse cracks observed on deck slab soffit area

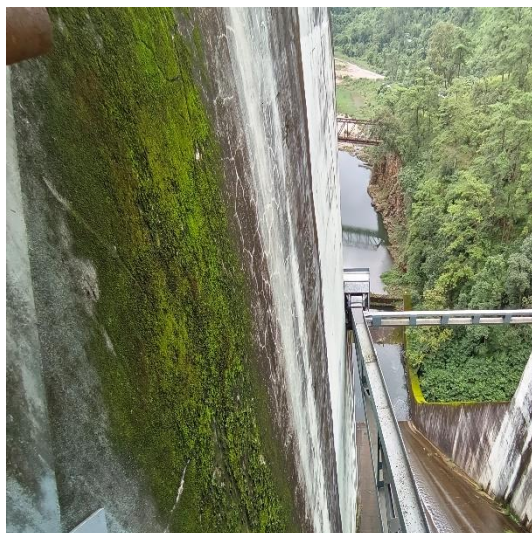


Silt accumulation, Vegetation growth observed on bearing junctions

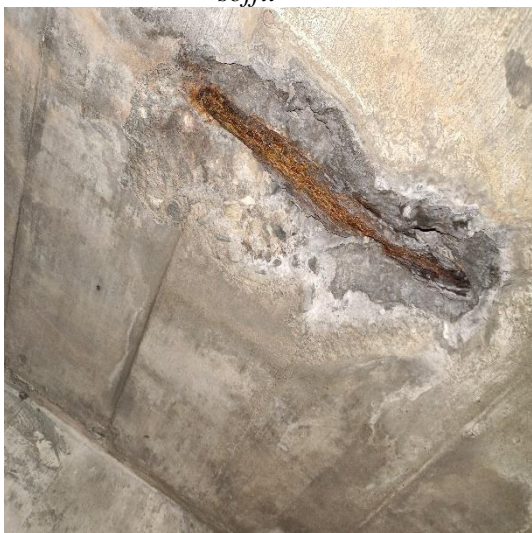
Figure 15: Observations on East side Abutment-2 and Pier-1 (Continue in Page: 15-18)



Spalling & Seepages sign observed on deck slab soffit



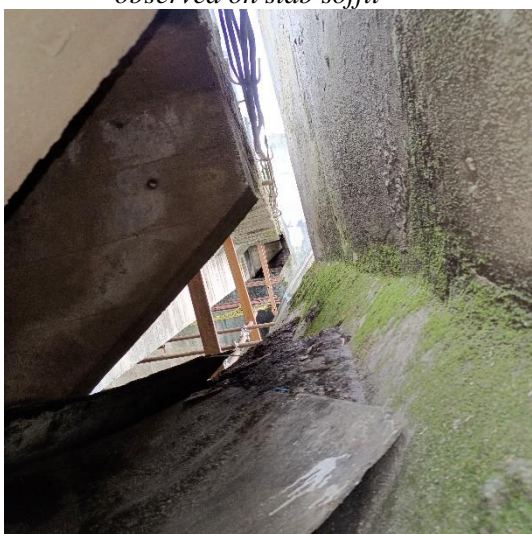
Major Seepages sign, Discoloration, vegetation growth observed on spillway wall



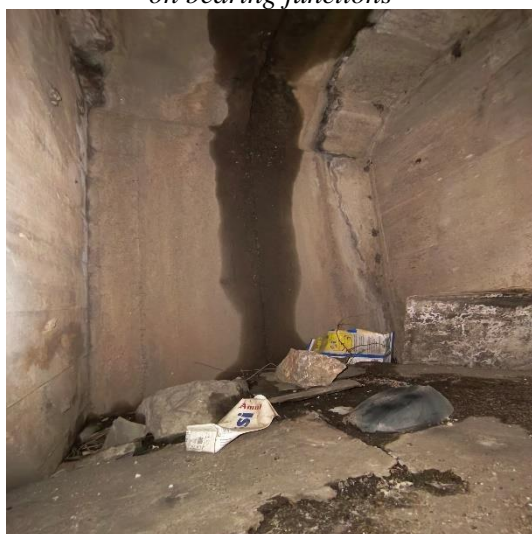
Spalling and corrosion in reinforcement observed on slab soffit



Silt accumulation & Major corrosion observed on bearing junctions



Seepages sign observed on cross girders



Seepages sign on deck slab & cracks observed on diaphragm wall

Figure 15: Observations on East side Abutment-2 and Pier-1 (Continue in Page: 15-18)



Spalling observed on cross girder



Shear cracks observed on girders



Vertical cracks observed on spillway wall

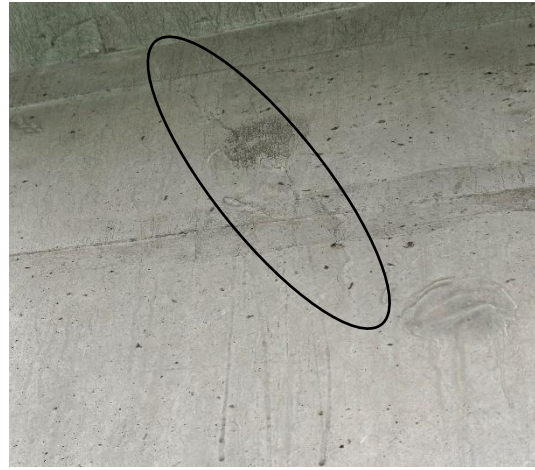


Severe rusting and silt accumulation observed on bearing junctions

Figure 15: Observations on East side Abutment 2 and Pier1



Repair in patches observed on beam surface



Shear cracks observed on girder beam



Transverse Cracks observed on deck slab soffit



Seepages signs observed on deck slab soffit



Seepages sign & discoloration observed on slab soffit surface



Longitudinal cracks observed on pier surface area

Figure 16: Observations on South side Abutment-2 and Pier-1



Transverse cracks and seepages sign observed on deck slab surface area



Shear cracks observed on girder beam



Vegetation growth & silt accumulation on pier cap

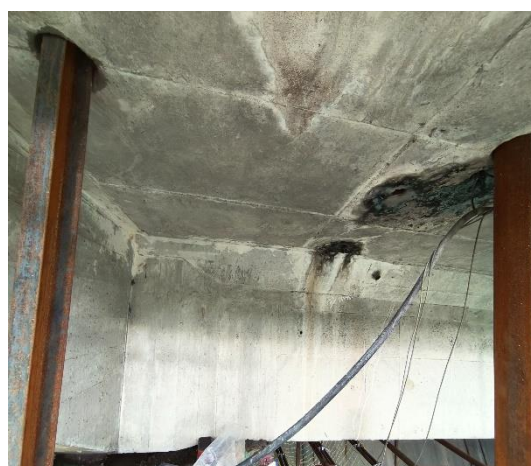


Spalling observed on pier cap surface area

Figure 17: Observations on West side Abutment-1 and Pier-1



Silt accumulation observed on bearing junctions



Seepages sign observed deck slab soffit

Figure 18: Observations on East and North Pier-1



Vegetation growth, Seepages signs & silt accumulation observed on bearing junctions



Shear cracks observed on girder beam.



Major Corrosion & vegetation growth observed on bearing



Vertical cracks observed on cross girders

Figure 19: Observations on North side Abutment-1 and Pier-1



No major corrosion observed on steel



No major corrosion observed on steel

Figure 20: Observations on East side deck slab and South side diaphragm wall



No major rusting observed on steel



Minor rusting observed on steel

Figure 21: Observations on South side deck slab and North side girder beam

After a thorough visual investigation of various parts of the bridge, some elements were found in distress condition. The general observations from this investigation are mentioned as bullet points as follows.

1. Shear cracks were observed on girder beams.
2. Transverse cracks were observed on the deck slab.
3. A seepage sign was observed on the deck slab soffit surface area.
4. Spalling & corrosion in steel observed on slab soffit and pier cap surface area.

5. Vegetation growth was observed on the pier cap.
6. Silt accumulation was observed on the pier cap near bearing junctions.
7. Severe corrosion in bearing and blocking was observed near junctions.
8. Longitudinal cracks were observed on the spillway wall.
9. Major seepages sign, discoloration and vegetation growth were observed on the pier cap surface area & spillway wall surface area.
10. Vertical cracks & seepages sign were observed on the diaphragm wall & cross girder.
11. Silt Deposition was observed on expansion joints near the bearing junction.
12. Major Seepages sign and hollowness were observed on the deck slab soffit nearby spouts.

1.4.2 Rebound Hammer Results

The rebound hammer test was carried out in thirty-four different locations on the bridge. Table 3 shows the rebound hammer test results. Based on this result, data has been processed and presented as (a) rebound value distribution, (b) concrete layer quality, and (c) concrete compressive strength, which are shown in Figures 22-24, respectively.

Table 3: Rebound hammer test results

Sl. No	Member	Level	Location	Rebound Hammer										Direction	MPa
				1	2	3	4	5	6	7	8	9	Avg.		
1	Girder Beam	A2	1	44	42	41	43	45	44	46	48	49	45	H	51
2	Slab	A2-P1	2	42	41	42	40	41	44	42	40	42	42	V Up	37
3	Abutment Cap	A2	3	48	40	42	38	40	42	39	42	38	41	H	45
4	Beam	A2	4	44	43	46	45	41	42	40	43	45	43	H	49
5	Slab	A2	5	48	46	45	43	44	45	49	48	47	46	V Up	46
6	Beam	A2	6	48	46	45	42	44	45	46	45	44	48	H	59
7	Cap	A2	7	40	42	43	44	45	42	43	45	42	43	V Up	36
8	Diaphragm wall	A2	8	42	45	46	48	44	45	49	48	47	46	H	53
9	Beam	P1-A2	9	45	46	48	45	46	47	46	48	45	46	H	53
10	Diaphragm wall	P1-A2	10	46	48	45	43	44	49	44	42	45	45	H	53
11	Slab	P1-A2	11	48	49	45	46	48	49	48	46	47	47	V Up	48
12	Cross Girder	P1-A2	12	40	39	42	44	38	46	45	42	40	42	H	45
13	Beam	P1-A2	13	40	44	41	43	45	40	44	46	41	43	H	47
14	Slab	P1-A2	14	44	48	45	46	49	48	44	45	46	46	H	53
15	Beam	P1-A2	15	48	45	44	46	50	48	46	45	48	47	H	53
16	Pier Cap	P1-A2	16	48	44	46	45	48	45	46	40	42	45	V Up	42
17	Diaphragm wall	P1	17	40	41	43	42	40	42	41	42	43	42	H	45
18	Corbel	P1	18	39	40	41	42	43	44	40	42	39	41	H	45
19	Slab	P1-A3	19	48	47	49	50	48	47	49	48	47	48	V Up	50
20	Beam	P1-A3	20	44	45	46	44	42	44	48	44	42	44	H	51
21	Slab	P1-A3	21	48	50	49	48	50	50	46	49	48	49	V Up	50
22	Diaphragm wall	P1-A3	22	49	50	48	48	47	50	51	47	51	49	H	61
23	Pier Cap	P1-A3	23	44	40	41	42	42	40	42	44	46	42	H	47
24	Slab	P1-A3	24	50	48	44	46	48	50	51	47	52	48	V Up	50
25	Diaphragm wall	P1	25	40	41	42	40	40	42	40	46	42	42	H	45
26	Beam	P1-A3	26	46	44	42	46	48	42	46	48	42	45	H	51
27	Cross Girder	P1-A3	27	42	41	46	42	44	42	46	45	42	43	H	49
28	Beam	A3	28	40	42	46	47	48	45	46	42	46	45	H	51
29	Slab	A3	29	42	46	45	45	43	48	49	47	45	46	V Up	44
30	Beam	A3	30	46	48	45	48	49	47	46	45	48	47	H	53
31	Diaphragm wall	A3	31	46	45	48	41	42	48	49	49	46	46	H	53
32	Slab	A3	32	45	46	47	46	44	48	47	48	49	47	V Up	46
33	Beam	A3	33	45	46	47	44	48	47	48	49	50	47	H	57
34	Pier Cap	A3	34	46	45	40	42	44	46	48	47	49	45	H	53
AVERAGE													45		49
MINIMUM													41		36
MAXIMUM													49		61

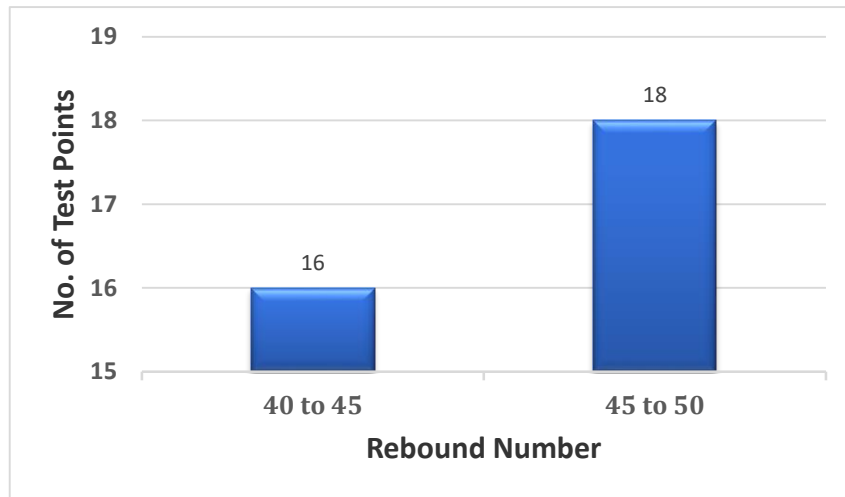


Figure 22: Distribution of rebound numbers measured

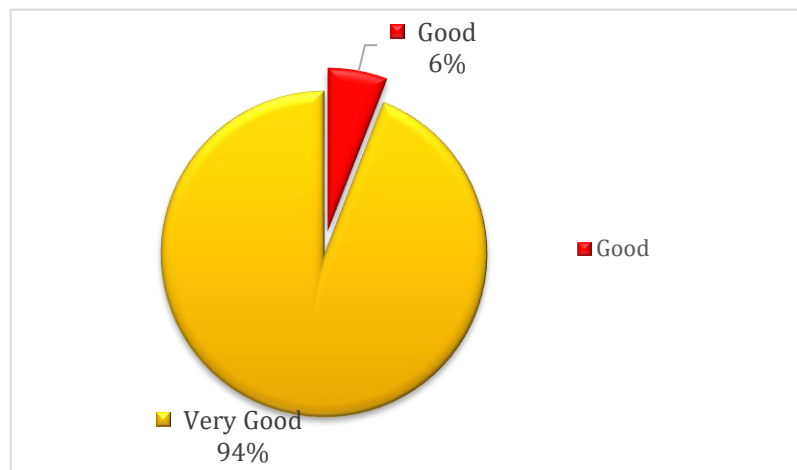


Figure 23: Estimated concrete layer quality based on rebound values

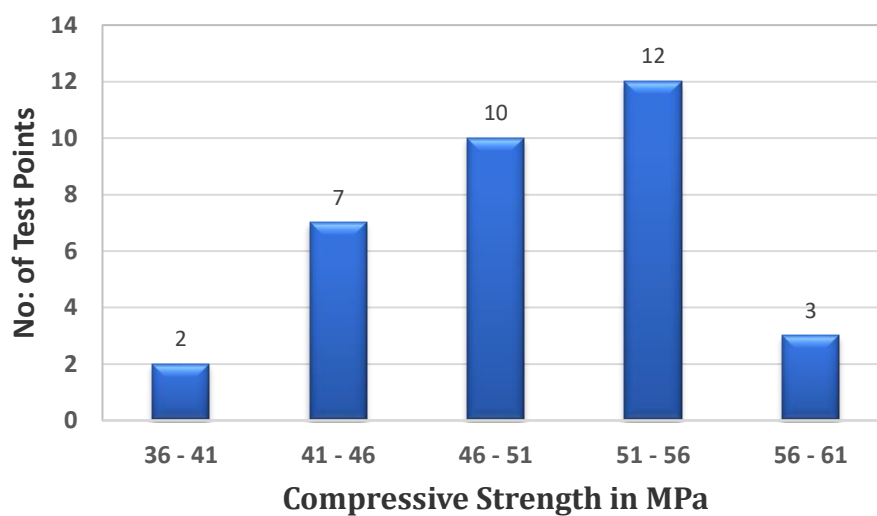


Figure 24: Estimated compressive strength based on rebound hammer test

1.4.3 UPV Results

Different fifty-four locations on the bridge components have been tested under the UPV test. The velocity criterion for concrete quality grading as per IS 516 is shown in Table 1. Based on the given velocity criteria, UPV test results are interpreted in Table 4. These processed data's are presented as (a) distributed form and, (b) concrete quality, which are shown in Figures 25 and 26, respectively.

Table 4: Ultrasonic pulse velocity test results

Sl. No.	Member	Level	Location	U.P. V				
				Dist. (m)	Time (μs)	Velocity (km/sec)	Quality	Method
1	Girder Beam	A2	1	0.46	113.00	4.07	Good	DIRECT
2	Girder Beam	A2	1	0.46	115	4.00	Good	DIRECT
3	Slab	A2-P1	2	0.40	102	4.42	Good	INDIRECT
4	Slab	A2-P1	2	0.40	114	4.01	Good	INDIRECT
5	Abutment Cap	A2	3	0.33	95	3.97	Good	INDIRECT
6	Beam	A2	4	0.46	122	3.77	Good	DIRECT
7	Beam	A2	4	0.46	118	3.90	Good	DIRECT
8	Slab	A2	5	0.40	105	4.31	Good	INDIRECT
9	Slab	A2	5	0.40	115	3.98	Good	INDIRECT
10	Beam	A2	6	0.46	125	3.68	Doubtful	DIRECT
11	Beam	A2	6	0.46	117	3.93	Good	DIRECT
12	Pier Cap	A2	7	0.40	115	3.98	Good	INDIRECT
13	Diaphragm wall	A2	8	0.39	75	5.70	Excellent	INDIRECT
14	Diaphragm wall	A2	8	0.39	88	4.93	Excellent	INDIRECT
15	Beam	P1-A2	9	0.46	122	3.77	Good	DIRECT
16	Diaphragm wall	P1-A2	10	0.40	100	4.50	Good	INDIRECT
17	Diaphragm wall	P1-A2	10	0.40	88	5.05	Excellent	INDIRECT
18	Slab	P1-A2	11	0.39	85	5.09	Excellent	INDIRECT
19	Slab	P1-A2	11	0.39	94	4.65	Excellent	INDIRECT
20	Cross Girder	P1-A2	12	0.43	111	4.37	Good	INDIRECT
21	Beam	P1-A2	13	0.46	114	4.54	Excellent	INDIRECT
22	Slab	P1-A2	14	0.40	130	3.58	Doubtful	INDIRECT
23	Slab	P1-A2	14	0.40	113	4.04	Good	INDIRECT
24	Beam	P1-A2	15	0.46	123	3.74	Doubtful	DIRECT
25	Beam	P1-A2	15	0.46	121	3.80	Good	DIRECT
26	Pier Cap	P1-A2	16	0.40	108	4.20	Good	INDIRECT
27	Diaphragm wall	P1	17	0.40	105	4.31	Good	INDIRECT
28	Diaphragm wall	P1	17	0.40	99	4.54	Excellent	INDIRECT
29	Corbel	P1	18	0.37	88	4.20	Good	DIRECT
30	Slab	P1-A1	19	0.39	118	3.81	Good	INDIRECT
31	Slab	P1-A1	19	0.40	122	3.78	Good	INDIRECT
32	Beam	P1-A1	20	0.46	124	3.71	Doubtful	DIRECT

Sl. No.	Member	Level	Location	U.P. V				
				Dist. (m)	Time (μs)	Velocity (km/sec)	Quality	Method
33	Slab	P1-A1	21	0.40	103	4.38	Good	INDIRECT
34	Slab	P1-A1	21	0.43	120	4.08	Good	INDIRECT
35	Diaphragm wall	P1-A1	22	0.40	99	4.54	Excellent	INDIRECT
36	Diaphragm wall	P1-A1	22	0.36	108	3.83	Good	INDIRECT
37	Pier Cap	P1-A1	23	0.40	128	3.63	Doubtful	INDIRECT
38	Slab	P1-A1	24	0.43	130	3.81	Good	INDIRECT
39	Slab	P1-A1	24	0.44	140	3.64	Doubtful	INDIRECT
40	Diaphragm wall	P1	25	0.41	106	4.37	Good	INDIRECT
41	Diaphragm wall	P1	25	0.41	101	4.56	Excellent	INDIRECT
42	Beam	P1-A1	26	0.46	122	4.27	Good	INDIRECT
43	Cross Girder	P1-A1	27	0.40	135	3.46	Doubtful	INDIRECT
44	Cross Girder	P1-A1	27	0.40	127	3.65	Doubtful	INDIRECT
45	Beam	P1-A1	28	0.46	121	3.80	Good	DIRECT
46	Slab	P1-A1	29	0.40	140	3.36	Doubtful	INDIRECT
47	Slab	P1-A1	29	0.40	130	3.58	Doubtful	INDIRECT
48	Beam	P1-A1	30	0.46	120	3.83	Good	DIRECT
49	Diaphragm wall	P1-A1	31	0.36	99	4.14	Good	INDIRECT
50	Diaphragm wall	P1-A1	31	0.35	87	4.52	Excellent	INDIRECT
51	Slab	P1-A1	32	0.40	119	3.86	Good	INDIRECT
52	Slab	P1-A1	32	0.40	114	4.01	Good	INDIRECT
53	Beam	P1-A1	33	0.40	113	3.54	Doubtful	DIRECT
54	Pier Cap	P1-A1	34	0.45	139	3.74	Doubtful	INDIRECT
AVERAGE						4.09		
MINIMUM						3.36		
MAXIMUM						5.70		

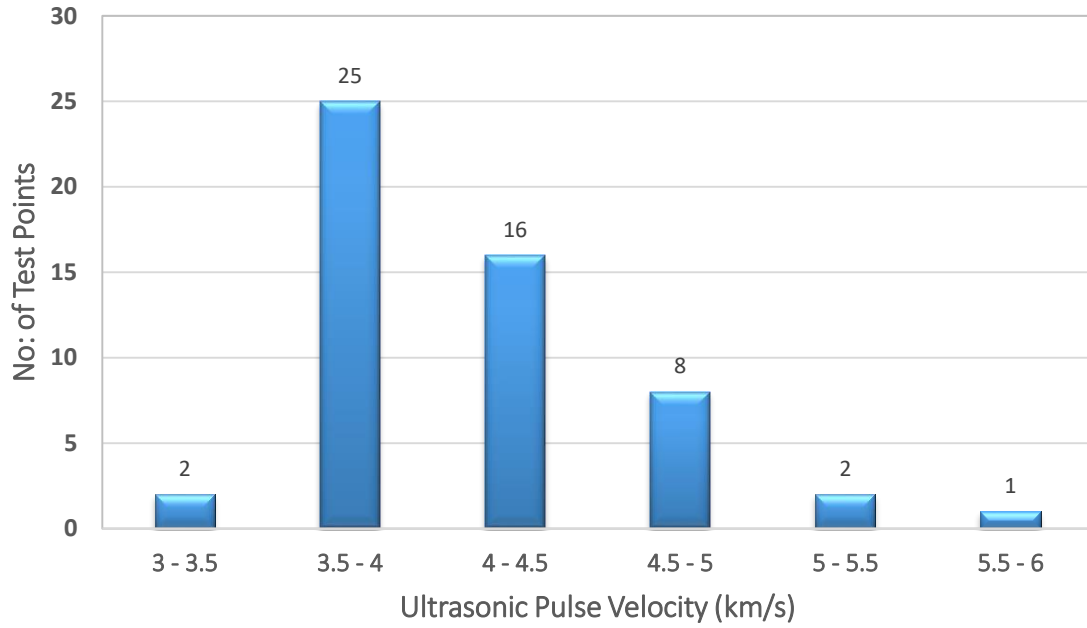


Figure 25: Distribution of measured UPV velocity

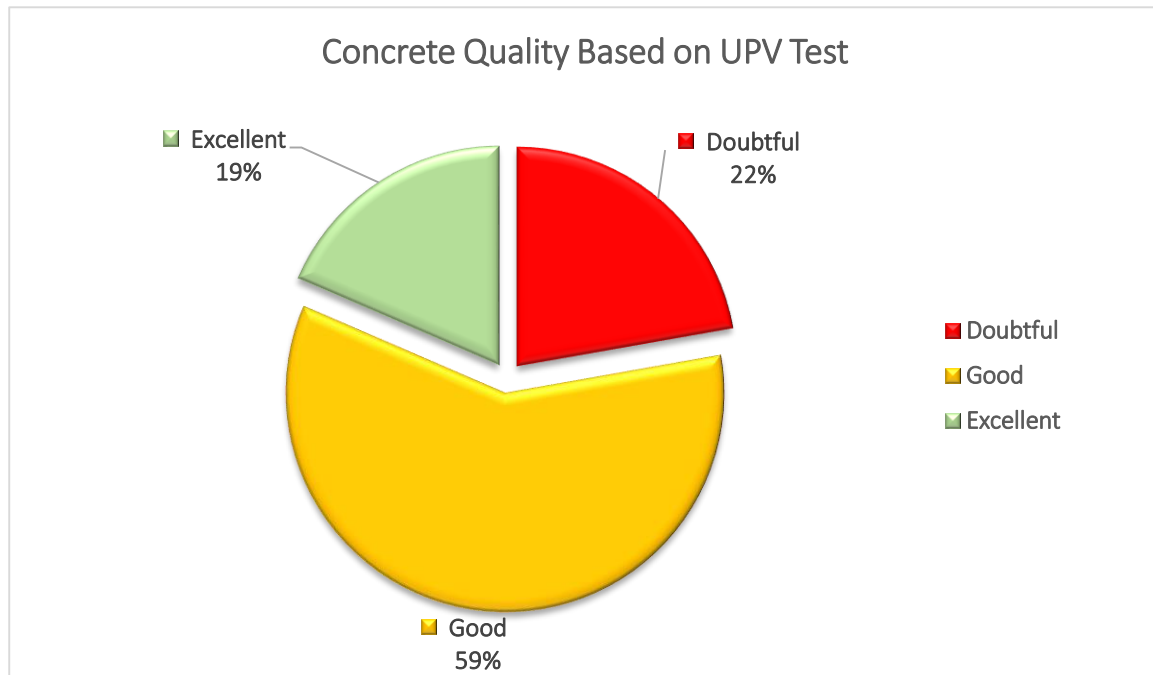











Figure 26: Estimated quality of concrete based on UPV test results

1.4.4 Core Compression Test Results

Five core samples have been taken from different locations of the bridge components with the help of a core-cutting machine. The compressive strength test on these core samples was carried out. Tables 5 and 6 show the sampling process of core cutting and compressive strength test results, respectively. Figures 27 and 28 show the distribution of compressive strength values estimated from the core compression test in the form of pie charts and bar charts.

Table 5: Core compressive test results

Sl. No	Core ID	Member Photo	Photo of Core Hole	Photo of Core After Capping	Visual Observation
Diaphragm Wall					
1	Core-01				Pores observed on sample.
Girder Beam					
2	Core-02				Pores observed on sample.
Pier Cap					
3	Core-03				Minor pores observed on sample.







Sl. No	Core ID	Member Photo	Photo of Core Hole	Photo of Core After Capping	Visual Observation
Girder Beam					
4	Core-04				Minor pores observed on sample
Girder Beam					
5	Core-05				Pores observed on sample.

Table 6: Concrete Compressive Strength (Core Test)

SL. No	Structure	Member Identification	Testing Date	Diameter D (mm)	Length L (mm)	L/D	Failure Load, (kN)	Core Strength (MPa)	Dia. Corr. Factor	L/D Corr. Factor	Corrected Compressive Strength of core (MPa)	Eqv. Cube Strength (MPa)
1	Diaphragm Wall	Core-1	31-07-2023	69.23	131.63	1.90	201.1	53.43	1.06	0.99	56.03	70.03
2	Girder Beam	Core-2	31-07-2023	69.24	133.73	1.93	133.0	35.33	1.06	0.99	37.16	46.45
3	Pier Cap	Core-3	31-07-2023	69.25	109.60	1.58	97.3	25.84	1.06	0.95	26.13	32.66
4	Girder Beam	Core-4	31-07-2023	69.26	129.31	1.87	115.1	30.55	1.06	0.99	31.91	39.89
5	Girder beam	Core-5	31-07-2023	69.25	132.69	1.92	72.8	19.33	1.06	0.99	20.30	25.38
Average												42.88

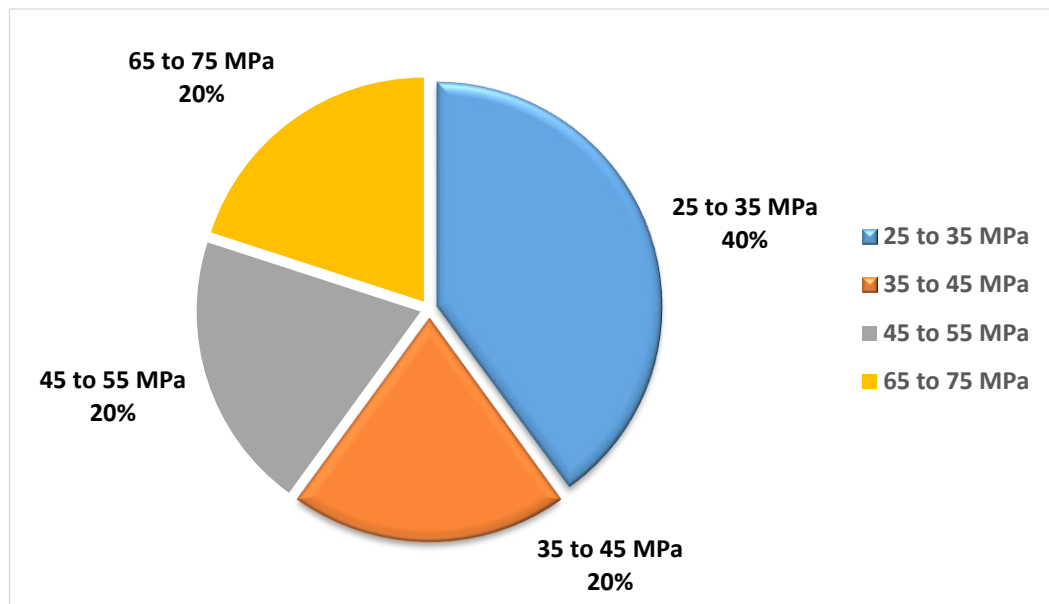


Figure 27: Distribution of compressive strength values estimated from core compression test

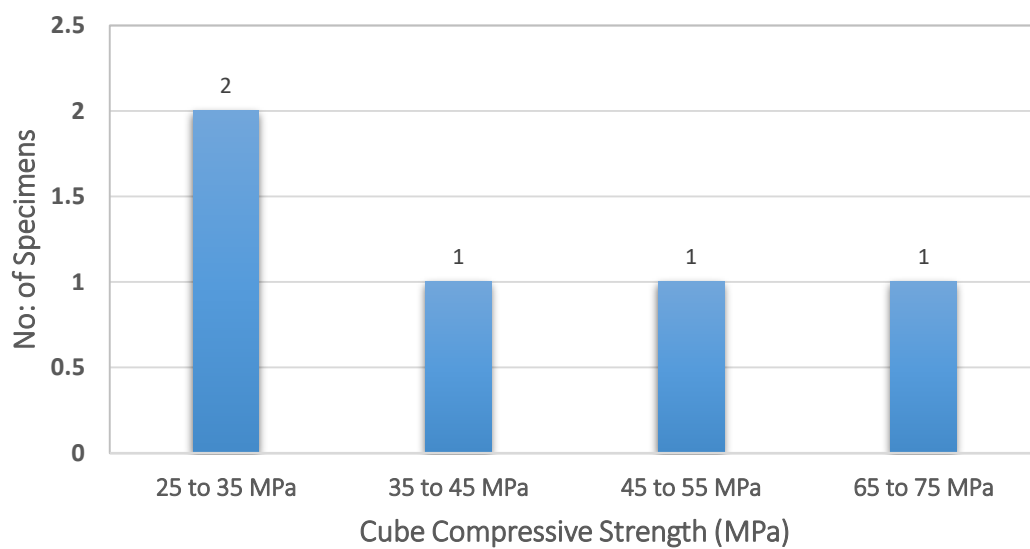


Figure 28: Core concrete compressive strength

1.4.5 Half-Cell Potential Test Results

In eleven different locations of the bridge component, the half-cell potential tests were carried out to identify the potential for corrosion. The probability of active corrosion ratings in the concrete are presented in the form of a table in Table 2, which was extracted from IS 516. Based on this rating, all half-cell potential data are analyzed and presented in the following table (i.e., Table 7). These analyzed data are presented in the distribution form in Figure 29. And the estimated corrosion probability is presented in the form of a Pie chart in Figure 30.

Table 7: Half-cell potential test results

Sl. No.	Member	Level	Location	Potential mV, (mili volts)					
				R1	R2	R3	R4	R5	Avg
1	Slab	A2-P1	2	-130	-158	-160	-140	-212	-160
2	Beam	A2	6	-140	-130	-150	-161	-143	-145
3	Diaphragm wall	A2	8	-118	-140	-117	-128	-150	-131
4	Cross Girder	P1-A2	12	-140	-160	-175	-161	-178	-163
5	Slab	P1-A2	14	-160	-140	-170	-180	-168	-164
6	Pier Cap	P1-A2	16	-150	-100	-180	-170	-161	-152
7	Pier Cap	P1-A1	23	-300	-310	-289	-273	-261	-287
8	Slab	P1-A1	24	-180	-178	-190	-210	-201	-192
9	Beam	P1-A1	28	-252	-220	-218	-215	-195	-220
10	Slab	P1-A1	29	-130	-168	-179	-200	-221	-180
11	Diaphragm wall	P1-A1	31	-185	-221	-230	-185	-201	-204
AVERAGE									-181
MINIMUM									-131
MAXIMUM									-287

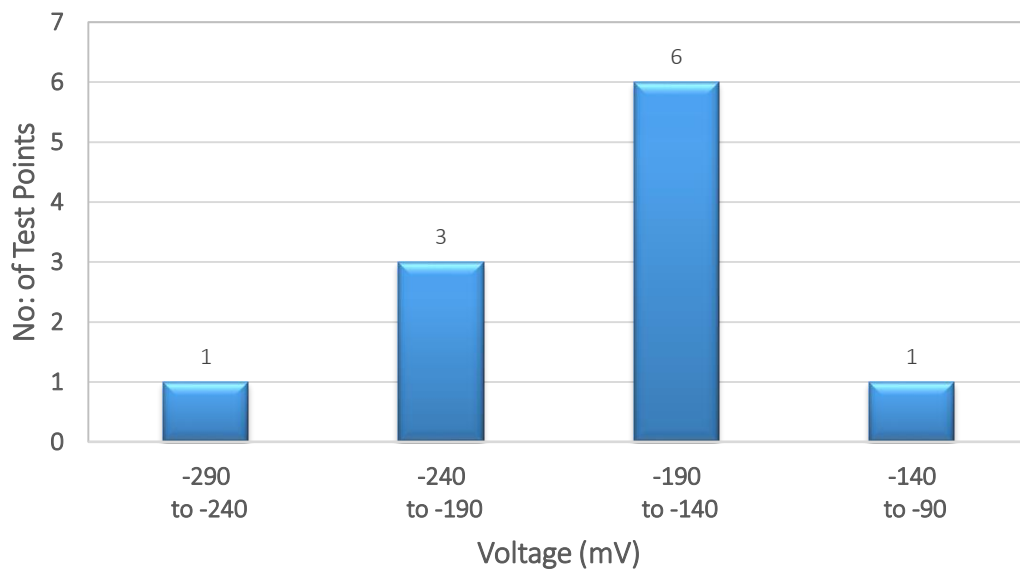


Figure 29: Distribution of half-cell potential values measured from the site

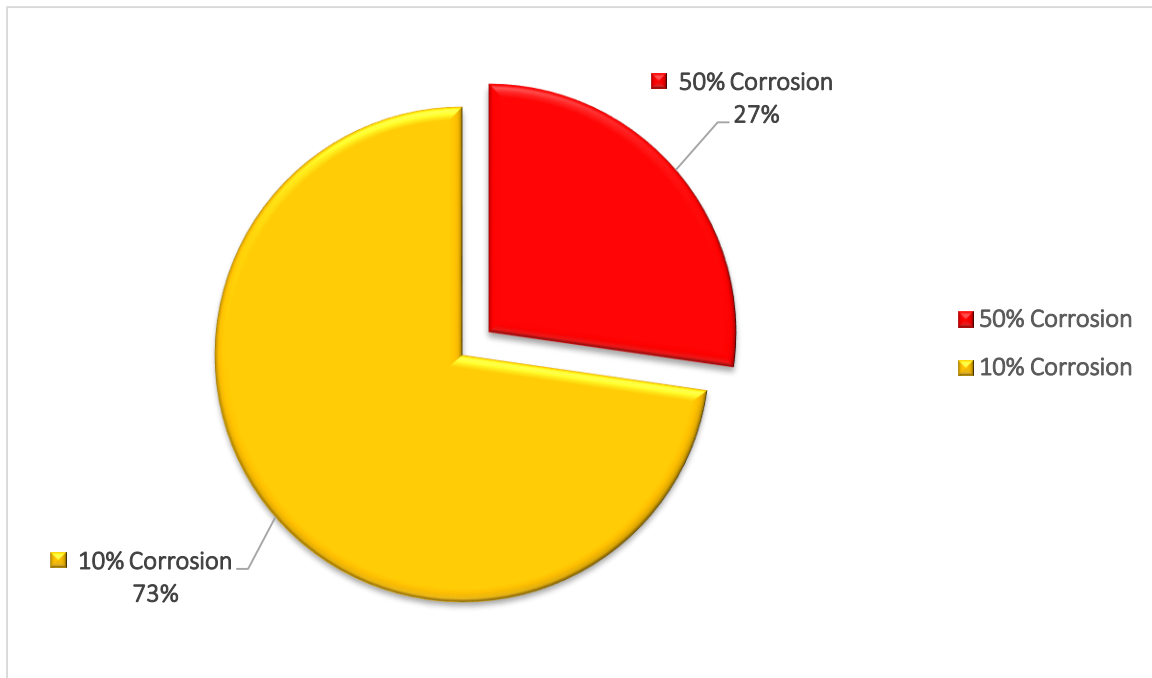


Figure 30: Estimated corrosion probability by half cell potential test

1.4.6 Carbonation Test Results

Carbonation test has been carried out in eleven different locations of the bridge components to assess the structure's durability and potential corrosion risk. The test results are presented in the form of a table in Table 8, and the depth of carbonation distribution is shown as a bar chart in Figure 31.

Table 8: Carbonation test results

Sr. No.	Member	Level	Location	Depth of Carbonation (mm)
1	Slab	A2-P1	2	10
2	Beam	A2	6	10
3	Diaphragm wall	A2	8	12
4	Cross Girder	P1-A2	12	12
5	Slab	P1-A2	14	10
6	Pier Cap	P1-A2	16	12
7	Pier Cap	P1-A1	23	15
8	Slab	P1-A1	24	12
9	Beam	P1-A1	28	12
10	Slab	P1-A1	29	10
11	Diaphragm wall	P1-A1	31	12
Average				12
Minimum				10
Maximum				15

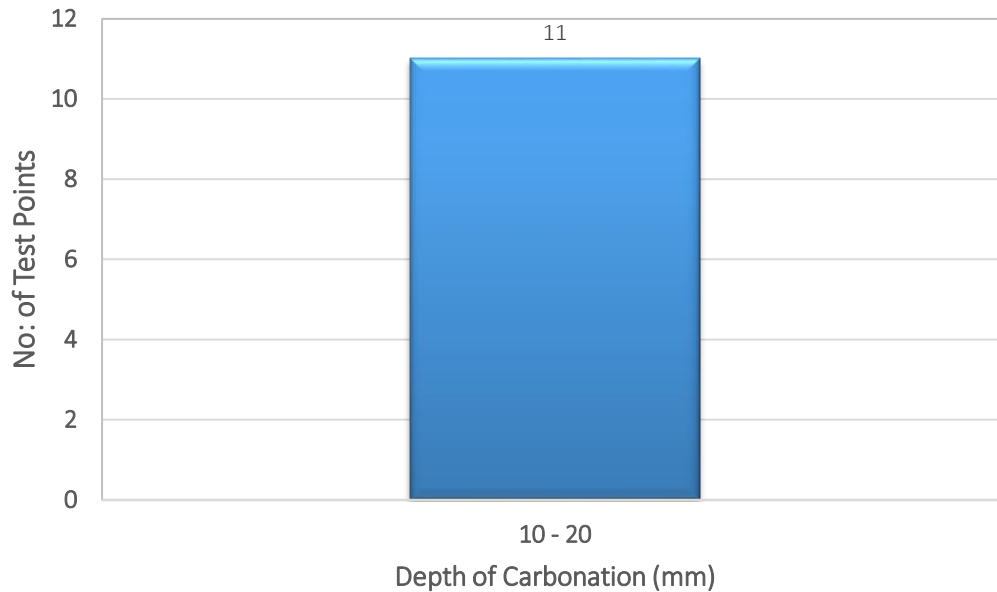


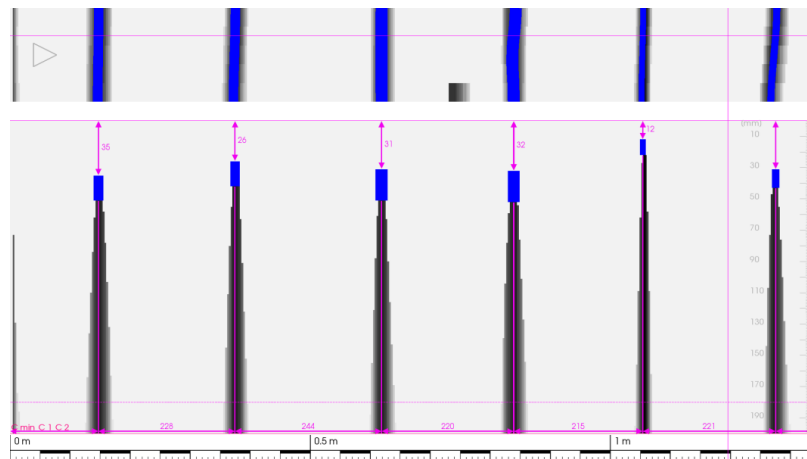
Figure 31: Distribution of depth of carbonation values obtained on various points

1.4.7 GPR Scanning Results

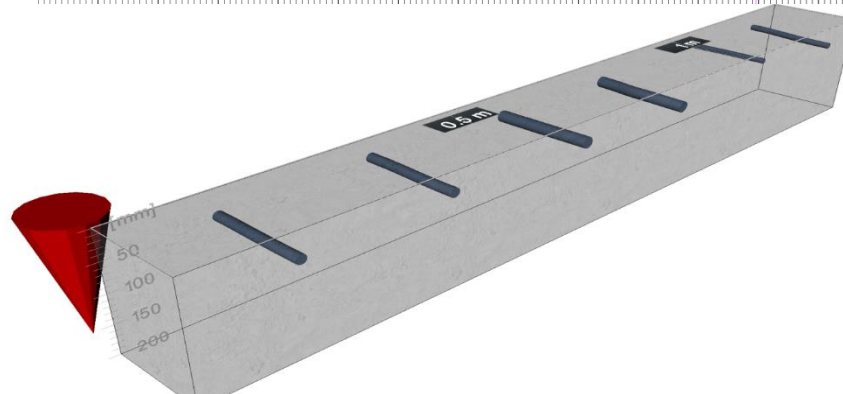
Ten different zones of the bridge component were tested using the GPR scanner to identify the cover concrete depth and reinforcement presence. Figures 32-41 show all GPR scanner report for each zone. Also, Table 9 summarises the overall GPR test results.

SCAN S1 (BEAM)

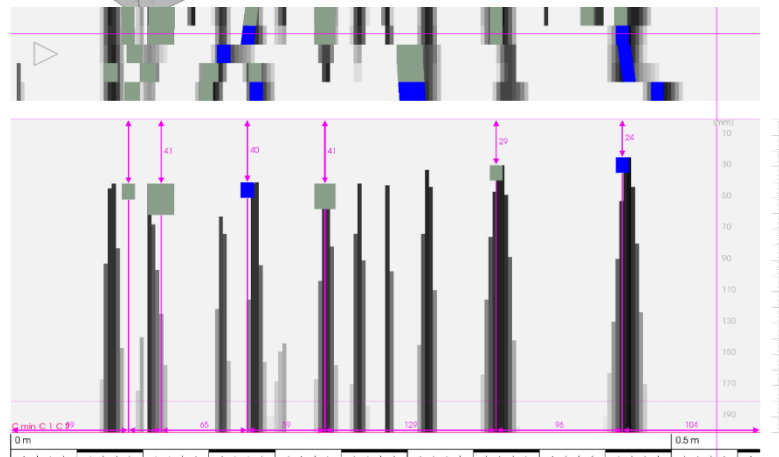
2D
View



3D View



2D
View



3D
View

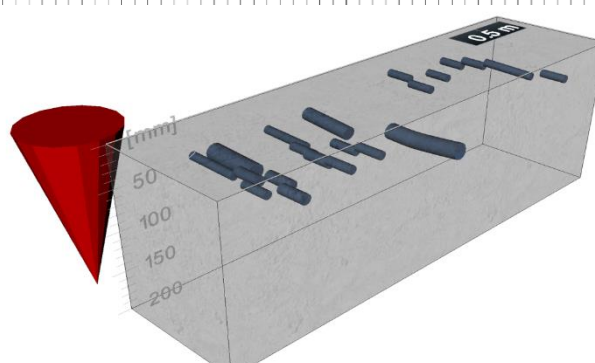


Figure 32: Rebar detection in scan-1 zone (beam)

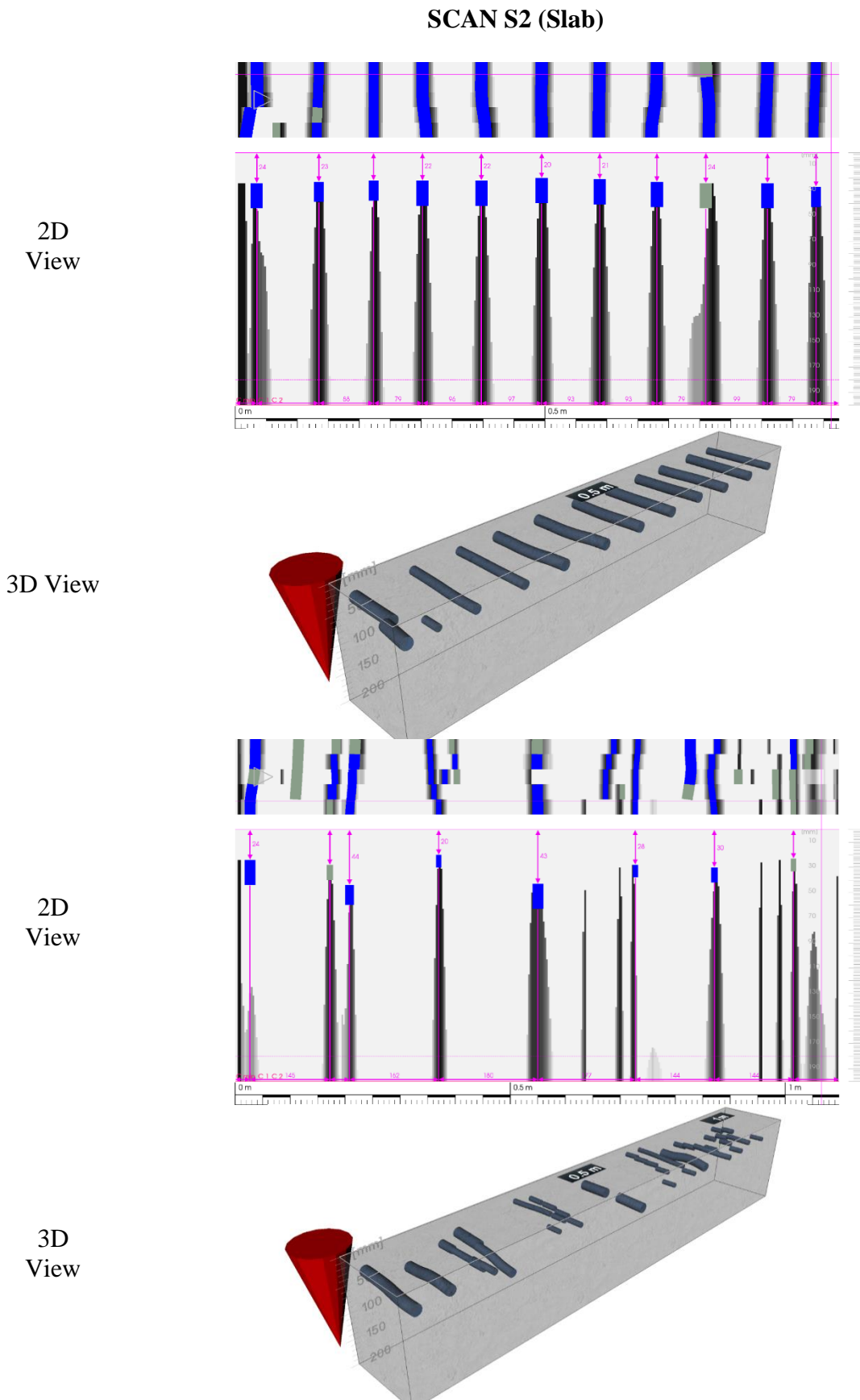
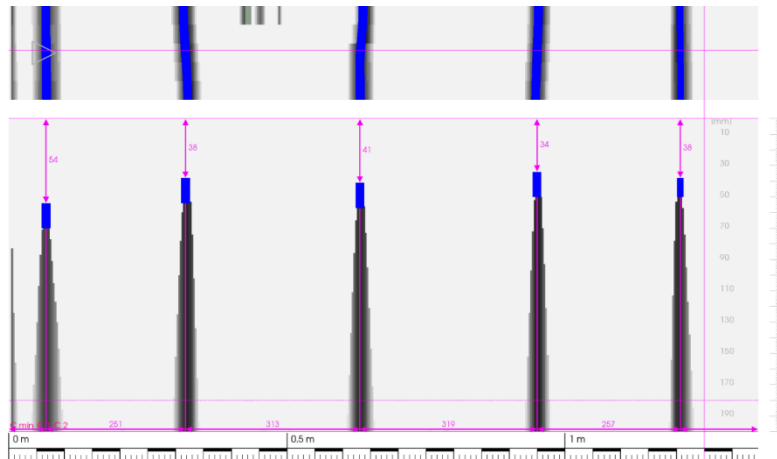


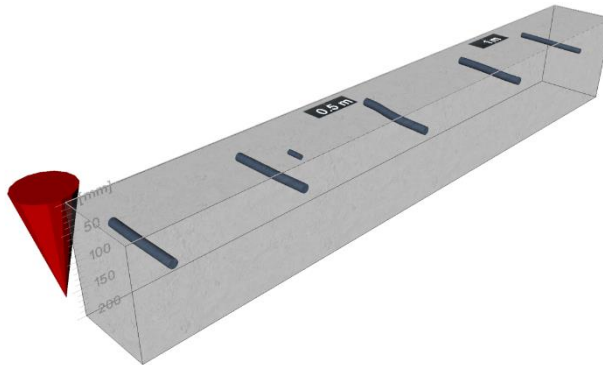
Figure 33: Rebar detection in scan-2 zone (slab)

SCAN S3 (Diaphragm Wall)

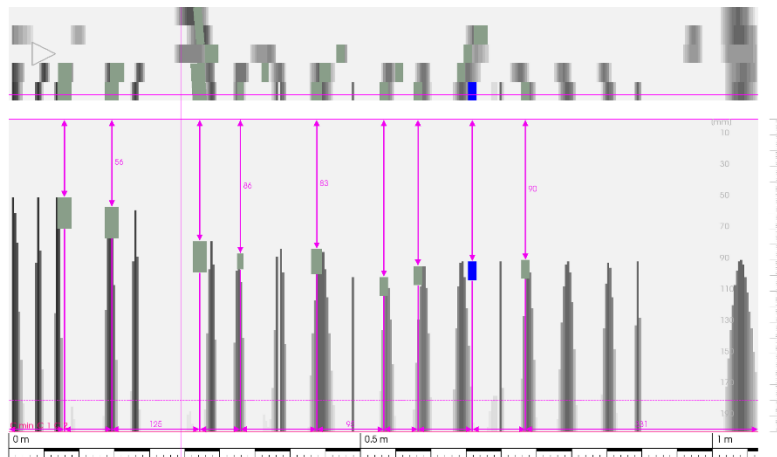
2D
View



3D View



2D
View



3D
View

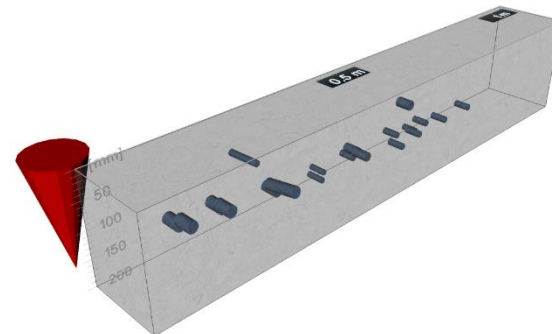
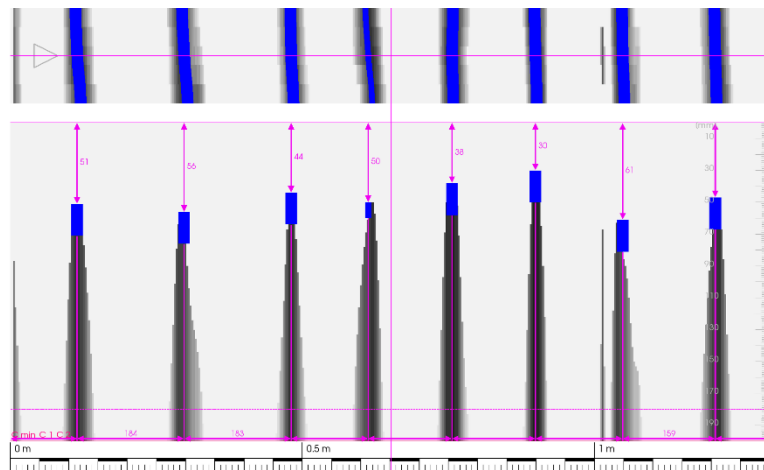


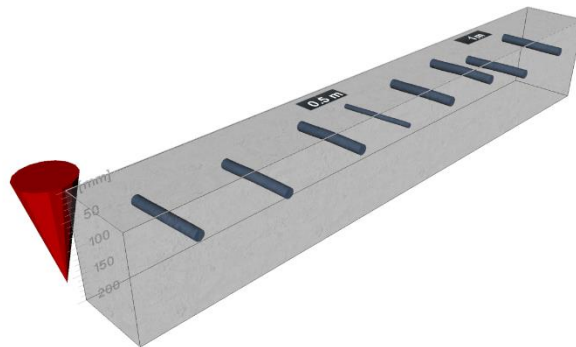
Figure 34: Rebar detection in scan-3 zone (diaphragm wall)

SCAN S4 (Pier Cap)

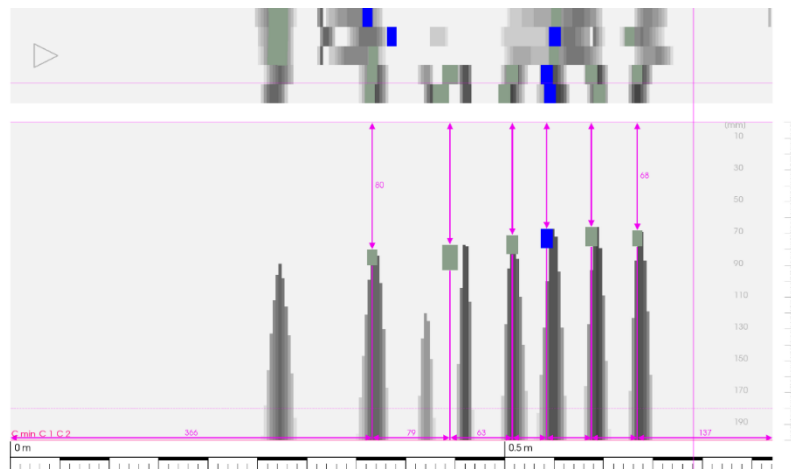
2D
View



3D View



2D
View



3D
View

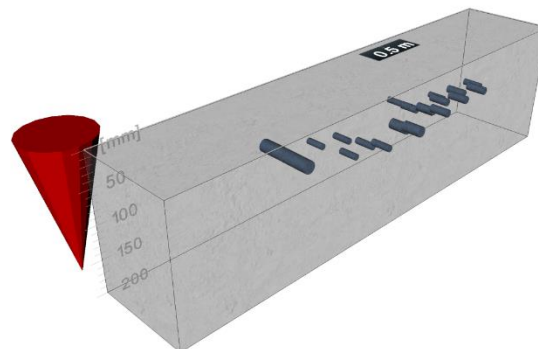
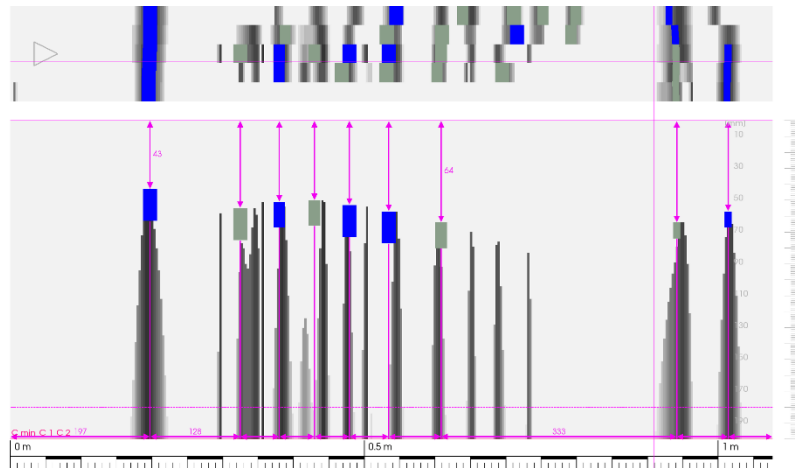


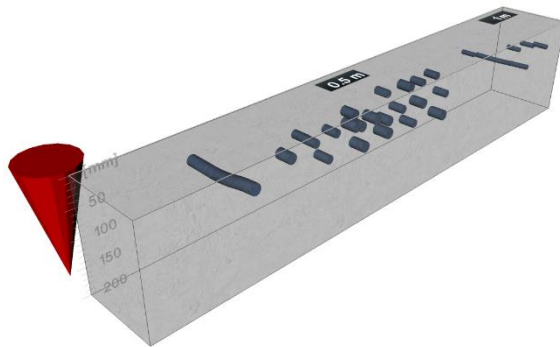
Figure 35: Rebar detection in scan-4 zone (Pier Cap)

SCAN S5 (Beam)

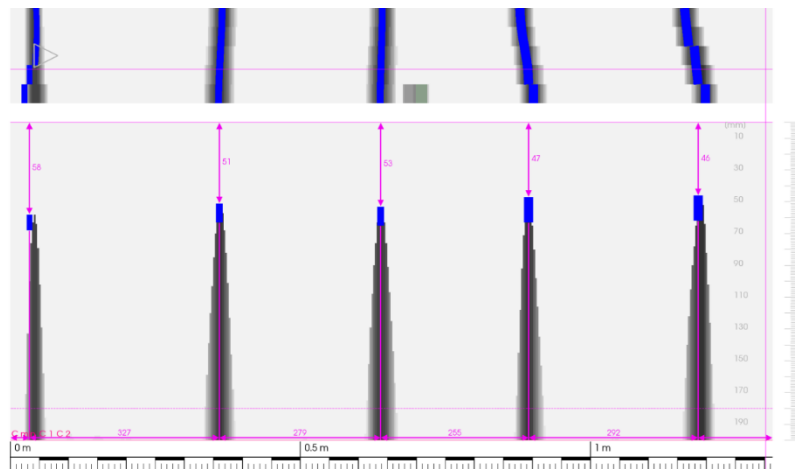
2D
View



3D View



2D
View



3D
View

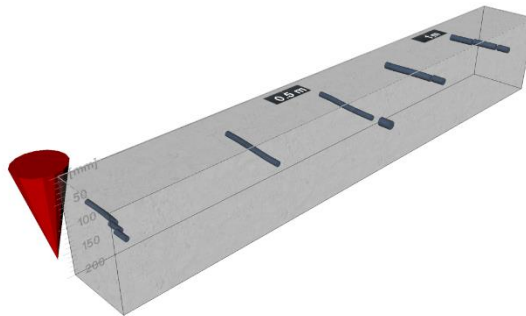


Figure 36: Rebar detection in scan-5 zone (beam)

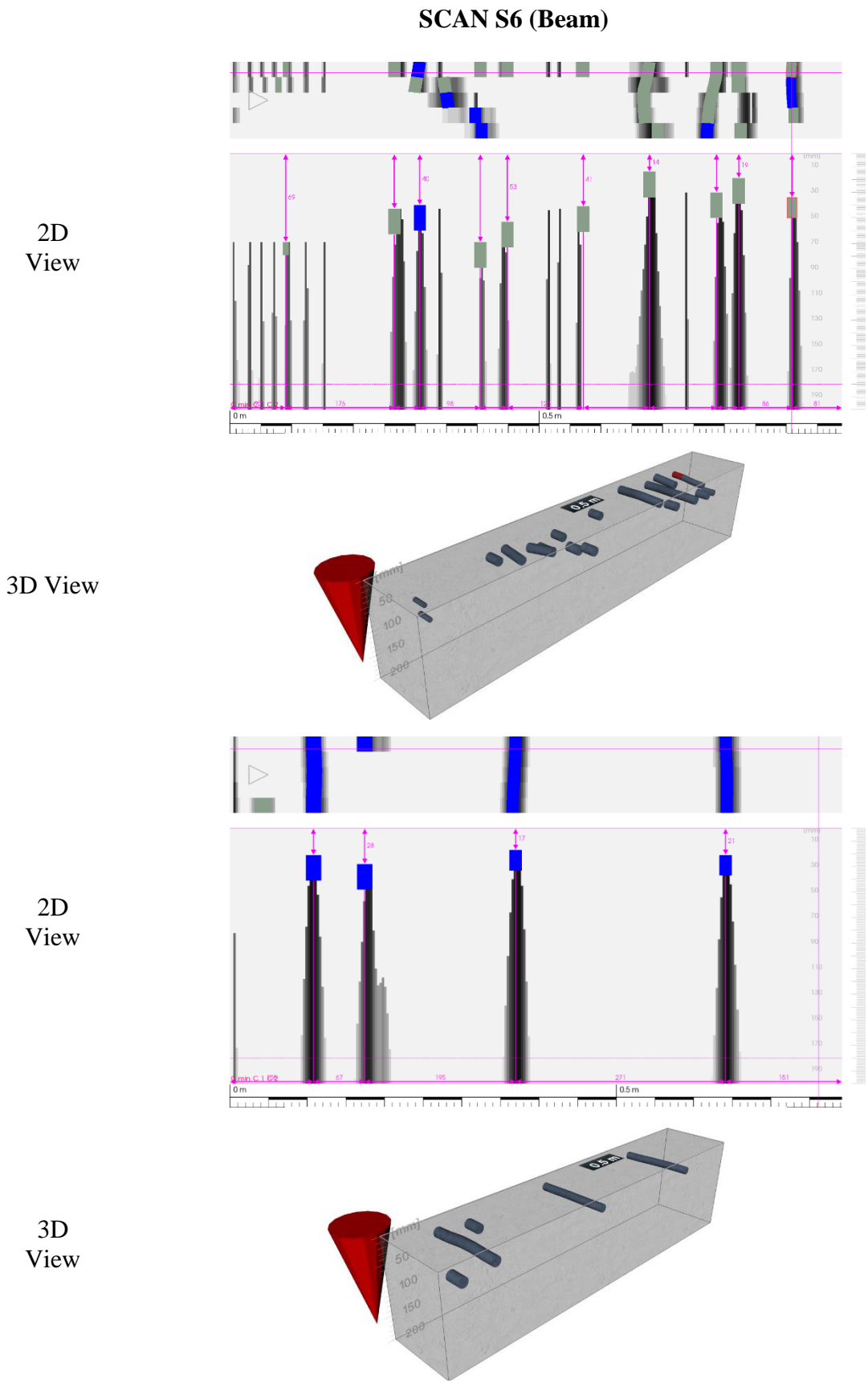
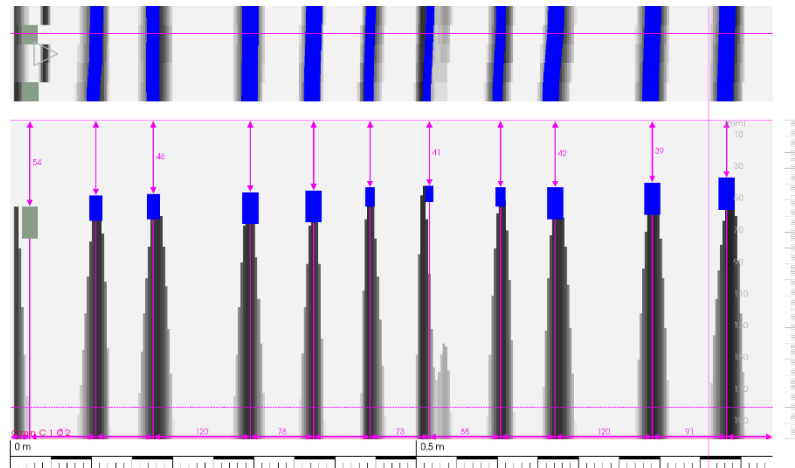


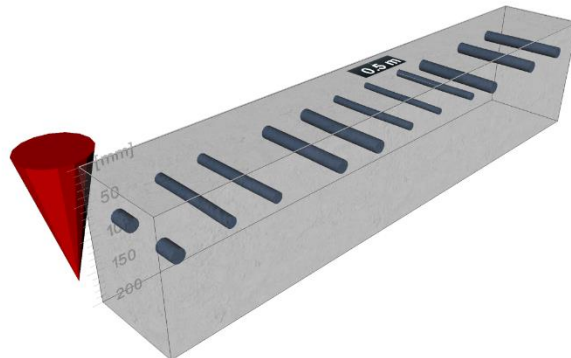
Figure 37: Rebar detection in scan-6 zone (beam)

SCAN S7 (Slab)

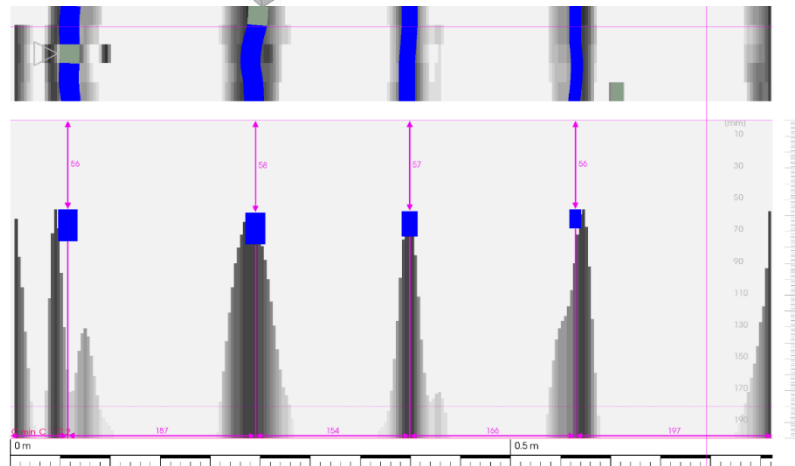
2D
View



3D View



2D
View



3D
View

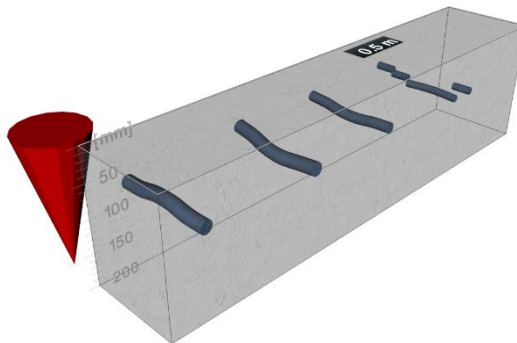
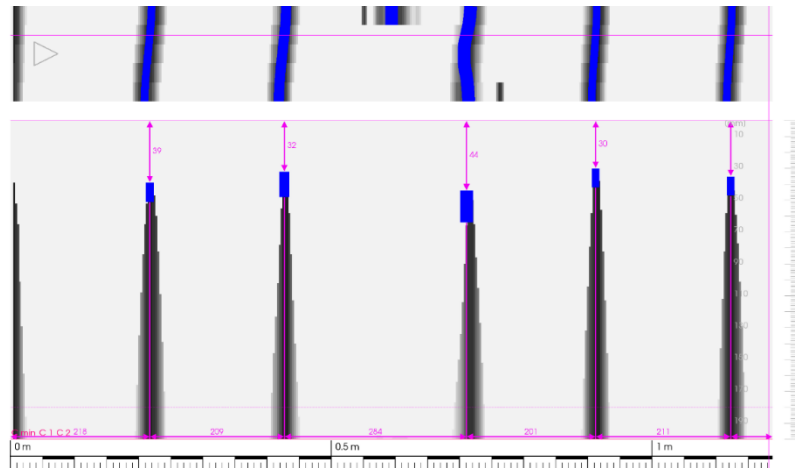


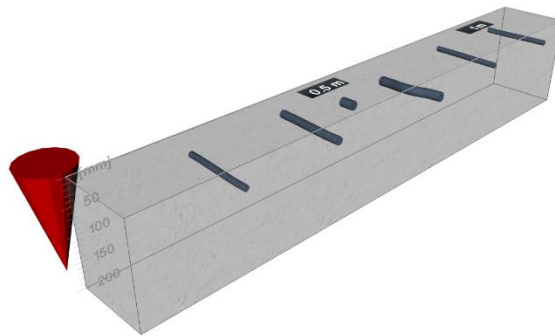
Figure 38: Rebar detection in scan-7 zone (slab)

SCAN S8 (Beam)

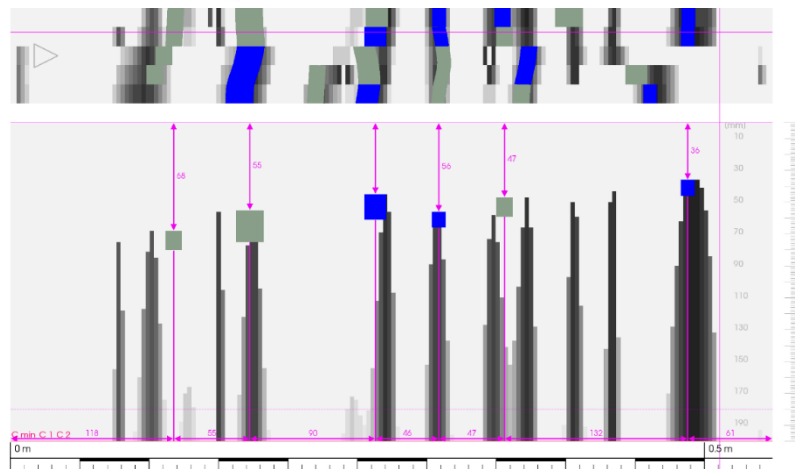
2D
View



3D View



2D
View



3D
View

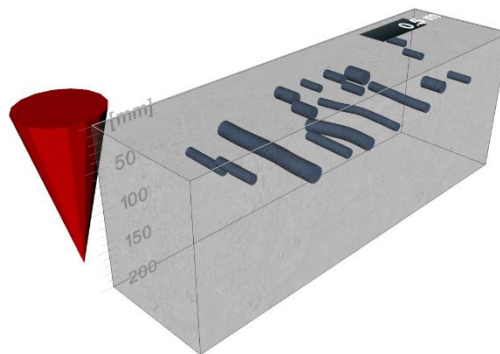
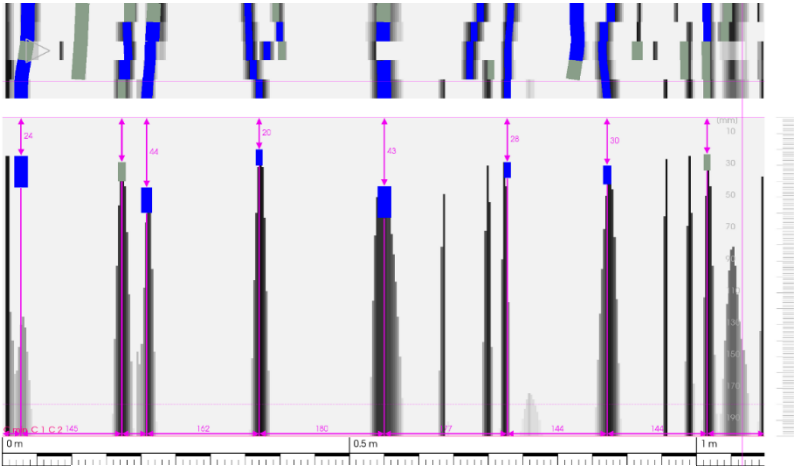


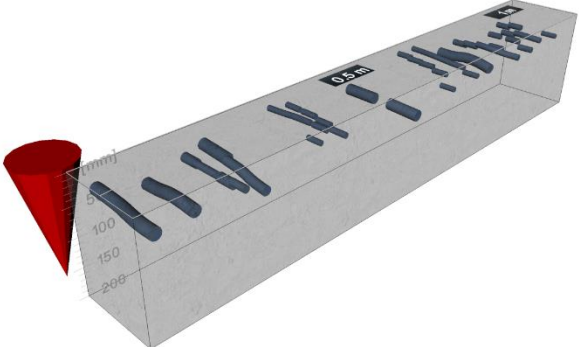
Figure 39: Rebar detection in scan-8 zone (beam)

SCAN S9 (Slab)

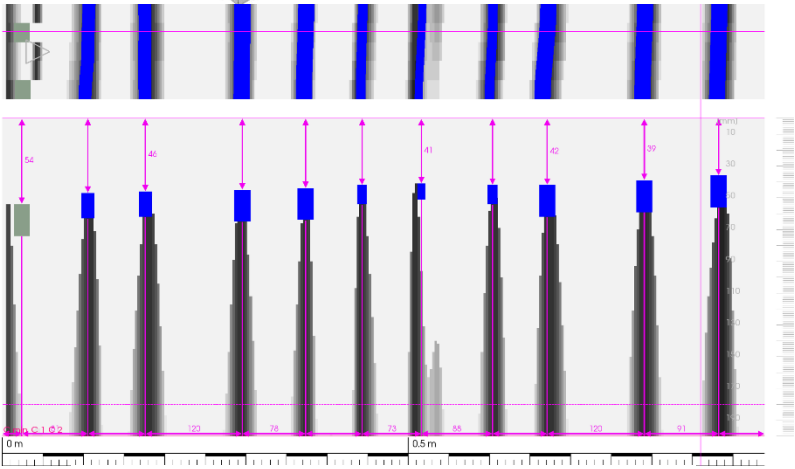
2D
View



3D View



2D
View



3D
View

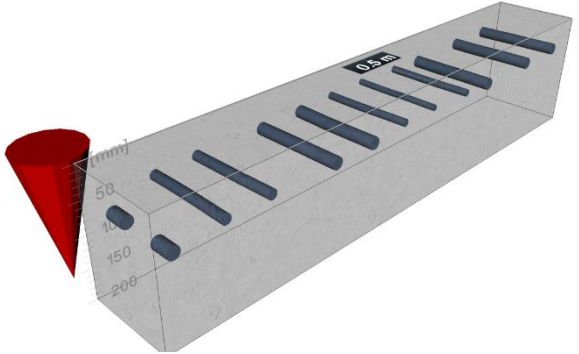
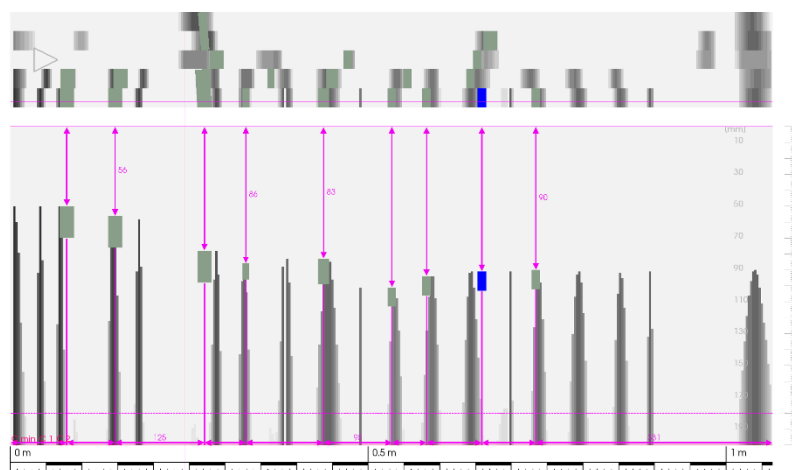


Figure 40: Rebar detection in scan-9 zone (slab)

Figure 41: Rebar detection in scan-10 zone (diaphragm wall)



A 3D schematic of a beam of length 1000 mm. A red cone representing a load is applied at the left end. The beam has a height of 100 mm and a width of 50 mm. A vertical scale on the left indicates distances of 50, 100, 150, and 200 mm. Four internal cracks are shown at different depths: 50 mm, 100 mm, 150 mm, and 200 mm. The cracks are labeled with their respective depths: 50 mm, 100 mm, 150 mm, and 200 mm.

Table 9: GPR test results

Sl. No	Scan Location	Clear Cover Upto (mm)	Type of Structure Component
1	S1	30	Beam
2	S2	25	Slab
3	S3	35	Diaphragm Wall
4	S4	48	Pier Cap
5	S5	32	Beam
6	S6	35	Beam
7	S7	24	Slab
8	S8	34	Beam
9	S9	26	Slab
10	S10	38	Diaphragm Wall

1.5 Conclusions

1.5.1 Visual Inspection

Visible structural and non-structural distresses were present. Severe Corrosion damages were observed on bearing junctions. Shear cracks on the girder beam & Transverse crack were observed on the deck slab. Moderate to Major distress was observed, which is highlighted in the report.

1.5.2 Rebound Hammer Test

The readings range from **36 MPa to 61 MPa**, and the average reading is **49 MPa**. Since the average readings are between **35-60 MPa**, indicating good concrete quality (IS 516: Part 5: Sec 4: 2020). Rebound Hammer results are fair quality, giving correlation for strength assessment. Due to the higher carbonation content in concrete, it gives overestimated strength.

1.5.3 UPV Test

The readings range from **3.36 km/sec to 5.70 km/sec**, and the average reading is **4.09 km/sec**. It is concluded that the average pulse passing through the concrete is above 3.75 km/sec; hence the concrete quality is GOOD (as per IS 516 Part 5/ Sec 1: 2018).

1.5.4 Core Compression Test

The equivalent compressive strength of the concrete core is **25.38 N/mm²** and **70.03 N/mm²**. It is concluded that the concrete quality is GOOD.

1.5.5 Half-Cell Potential Test

The average readings vary from -131 mV to -287 mV, indicating that the probability of active corrosion is approximately 10%. Half-cell potential gives the probability of active corrosion in reinforcement. Severe corrosion was observed in a few of the elements, which is highlighted.

1.5.6 Carbonation Test

The carbonation depth in RCC members is **10-15 mm**, and the average depth is **12 mm**. Carbonation test results specify that carbonation depth is up to concrete cover and some elements have high corrosion. In some of the RCC elements, carbonation depth is above cover due to corrosion.

1.5.7 GPR Test

All cover concrete depths of different structural components are acceptable as per IS 456:2000.

1.6 Recommendations

Based on the above-mentioned critical observations and findings, the following points are recommended:

- The bridge is in moderately good condition. Multiple shear cracks are observed on the girder beam & Transverse cracks on the deck slab. Also, moderate to major distress in the joint regions. Therefore, MeECL should further investigate the matter, as a separate task, with the operational/actual loading condition.
- Heavy trucks should not permit until retrofitting of distressed members (i.e., girder beam & deck slab).
- Lifting the bridge girder up to a permissible level, considering the stability of the structure, is acceptable to replace crucial bridge components like bearings or for repair purposes.

DISCLAIMER

1. This report is based on collected data from the actual site.
2. The test result relates only to the item tested. This report shall not be reproduced, except in full, without the written permission of IIT Guwahati.
3. Statement of conformity to a specification is provided considering the level of risk associated with the decision rule applied.
4. Measurement uncertainty is not taken into consideration.

ACKNOWLEDGMENT

The IIT Guwahati team sincerely thanks the MeECL team for their invaluable support in facilitating logistical arrangements and ensuring an uninterrupted power supply during the test. Their assistance played a pivotal role in the successful execution of this project. We appreciate their collaborative spirit and dedication, which greatly contributed to achieving our objectives effectively.
